HHS Public Access

Author manuscript

Cancer Discov. Author manuscript; available in PMC 2020 May 01.

Published in final edited form as:

Cancer Discov. 2019 November ; 9(11): 1520–1537. doi:10.1158/2159-8290.CD-19-0391.

Anti-tumor T-cell homeostatic activation is uncoupled from homeostatic inhibition by checkpoint blockade

Netonia Marshall[1], **Keino Hutchinson**[2], **Thomas U Marron**[1], **Mark Aleynick**[1], **Linda Hammerich**[1], **Ranjan Upadhyay**[1], **Judit Svensson-Arvelund**[1], **Brian D Brown**[3], **Miriam Merad**[1,4], **Joshua D Brody**[1,*]

[1]Department of Medicine, Division of Hematology and Medical Oncology, Icahn School of Medicine, Mount Sinai Hospital, New York, NY 100029, USA

[2]Pharmacological Sciences, Icahn School of Medicine, Mount Sinai Hospital, New York, NY 100029, USA

[3]Genetics and Genomic Sciences, Icahn School of Medicine, Mount Sinai Hospital, New York, NY 100029, USA

[4]Oncological Sciences, Icahn School of Medicine, Mount Sinai Hospital, New York, NY 100029, USA

Abstract

T-cell transfer into lymphodepleted recipients induces homeostatic activation and potentiates anti-tumor efficacy. In contrast to *canonical* TCR-induced activation, *homeostatic* activation yields a distinct phenotype and memory state whose regulatory mechanisms are poorly understood. Here, we show in patients and murine models that, following transfer into lymphodepleted bone marrow transplant (BMT) recipients, $CD8^+$ T-cells undergo activation but also simultaneous *homeostatic inhibition* manifest in upregulation of immune checkpoint molecules and functional suppression. T-cell transferred into BMT recipients were protected from homeostatic inhibition by PD1/CTLA4 dual checkpoint blockade (dCB). This combination of dCB and BMT–'immunotransplant'–increased T-cell homeostatic activation and anti-tumor T-cell responses by an order of magnitude. Like homeostatic activation, homeostatic inhibition is IL-7/IL-15-dependent, revealing mechanistic coupling of these two processes. Marked similarity in *ex vivo* modulation of post-BMT T-cell in mice and patients is promising for the clinical translation of immunotransplant (NCT03305445) and for addressing homeostatic inhibition in T-cell therapies.

Introduction

Lymphodepletive therapies, such as autologous bone marrow transplant (BMT) following high dose chemotherapy, improve survival in patients with lymphoma and are standard therapy for relapsed and/or refractory disease [1]. Despite this, aggressive lymphomas are incurable in ~10,000 people annually, indicating the need for novel therapies. Although

[*]**Correspondence:** Joshua Brody, 1470 Madison Ave, New York, NY 10029, USA. Joshua.Brody@mssm.edu.

No potential conflicts of interest are disclosed by the authors.

some lymphomas are sensitive to T-cell killing, as exemplified by the unprecedented efficacy of PD1-blockade in Hodgkin's lymphoma [2], checkpoint blockade has been largely ineffective in non-Hodgkins lymphomas (NHL). Even anti-PD1/anti-CTLA4 dual checkpoint blockade (dCB) has yielded limited efficacy (complete response rate 0%, median survival < 3 months) [3] despite higher intratumoral expression of response predictors (e.g., PDL1, CD8, IFNγ) in NHL compared to responsive tumor types [4]. This inefficacy may be due to insufficient T-cell activation. Previously, we improved checkpoint-blockade efficacy by cross-priming anti-lymphoma T-cells[5] to enhance their TCR-induced activation.

Homeostatic activation is triggered in mature T-cells upon their transfer into a lymphodepleted recipient and their increased access to common gamma chain (γ_c) cytokine family members IL-7 and IL-15, promoting anti-tumor responses [6]. In contrast to TCR-mediated activation, which occurs via ZAP70/Lck/LAT/MAPK/Erk signals [7], homeostatic activation is mediated by cytokine receptor signaling via Jak/STAT[8] resulting in distinct states of activation and exhaustion [9]. Lymphodepletion is necessary for the efficacy of cellular therapies and has been incorporated into T-cell transfer therapies, including CAR-T [10], TIL [11] and transgenic TCR therapy [12] as well as allogeneic BMT [13].

Both canonical TCR-mediated activation and homeostatic activation of T-cells result in proliferation and memory induction[14]. Canonical TCR-mediated activation and homeostatic activation share some common features but also numerous *differences*, e.g. homeostatic activation does *not* induce upregulation of CD25, CD69 and CD71 [15, 16] or downregulation of CD49d [17], CD62L [16], or CD127 [15]. While TCR-mediated activation increases PD-1 expression, other T-cell activators such IL-12 actually *decrease* PD-1 expression [18].

The effects of *homeostatic* activation on expression of checkpoint molecules and response to checkpoint ligands has not been well studied. Broadly, the regulation of homeostatic activation, the expression of checkpoint molecules on transferred T-cells, and the effect of checkpoint blockade in this setting, are poorly understood. Here, we show that transfer of both murine and human CD8+ T-cells into lymphodepleted recipients induces not only their activation but also expression of functional checkpoint molecules including CLTA-4 and PD-1 – we term this homeostatic inhibition.

Common gamma chain (γ_c) cytokine family members IL-7 and IL-15 are known to induce homeostatic proliferation [19, 20]; we further show that homeostatic inhibition is induced by IL-7 and IL-15 and JAK/STAT signaling. While homeostatic activation and inhibition are causally linked by the γ_c cytokines, we hypothesized that they could be effectively uncoupled by dCB. To test our hypothesis, we investigated the unconventional use of dCB during BMT. Our studies indicate that dCB protects transplanted T-cells from inhibitory signaling, and potentiates their homeostatic activation. This increased T-cell activation from the combination of BMT and dCB – termed 'immunotransplant' (IT) – significantly amplified anti-tumor immune responses yielding durable tumor regressions in lymphoma and solid tumors models, even when dCB alone yielded no apparent anti-tumor effect. These findings both reveal a novel T-cell regulatory mechanism and suggest a therapeutic approach

for checkpoint-refractory tumors, now being studied in patients with aggressive NHL (NCT03305445).

Results

Homeostatic activation is coupled to homeostatic inhibition in patients receiving autologous BMT

Standard autologous BMT re-infuses patients' peripheral blood mononuclear cells (PBMC) with mobilized stem cells after high dose chemotherapy. To determine the effects of lymphodepletion on patient T-cells, PBMC were isolated from patients prior to receiving BEAM (BCNU, etoposide, cytarabine, melphalan) chemotherapy (i.e., pre-transplant) and 7–10 days after autologous BMT (i.e., post-transplant). As expected, transfer of T-cells into lymphodepleted recipients lead to activation and proliferation of the CD4+ and CD8+ T-cells, as indicated by increased expression of the homeostatic activation markers CD44 and CD122/IL-2rβ [21]— and the proliferation marker Ki-67 staining (Fig. 1A and Supp. Fig. 1A). Interestingly, there was also 2- to 6-fold higher levels of PD1 and CTLA4 after reinfusion and expansion post lymphodepletion (Fig. 1B and Supp. Fig. 1B).

Expression of PD1 and CTLA4 on T-cells can mark activated or dysfunctional cells. To determine whether the increased checkpoint expression on post-transplant T-cells was functionally suppressive, we assessed T-cell stimulation with concurrent ligation of PD1 or CTLA4 by plate-bound PD-L1 or CD80. In the presence of checkpoint ligands, the stimulation of post-transplant $CD8^+$ T-cells, per their expression of activation markers and cytokines, was diminished as compared to matched pre-transplant samples (Fig. 1C and D). This transfer-induced, checkpoint-mediated suppression we termed *'homeostatic inhibition'*. Interestingly, transferred $CD4^+$ T-cells did not show the same diminished activation in the presence of PD-L1 or CD80 despite upregulation of PD1 and CTLA4 (Supp. Fig. 1C and D).

As an alternate source of checkpoint ligands than plate-bound PD-L1 and CD80, we developed a cell-based assay using Staphylococcal enterotoxin B (SEB) to aggregate antigen-presenting cells (APC) with T-cells and activate the latter. Here, SEB binding to T-cell-expressed TCR and APC-expressed MHC molecules co-localizes T-cell checkpoints with their ligands (e.g. PD-L1 and CD80) [22]. Pre- and post-transplant PBMCs were incubated with dCB, then stimulated with SEB and assessed for activation per their expression of IFNγ and CD25. As previously shown, homeostatic activation lowers the threshold for TCR activation [23]. Post-transplant $CD8^+$ T-cells were significantly more activated ($CD25^+$) by SEB than pre-transplant $CD8^+$T-cells (Fig. 1E *left panel,* pre- vs. post-transplant SEB, 27% vs 80%).

Surprisingly, although pre-transplant $CD8^+$ T-cells were activated with SEB, checkpoint blockade did *not* enhance this activation (Fig. 1E *left panel,* SEB vs. SEB+dCB, 27% vs. 29%). By contrast, post-transplant $CD8^+$ T-cell activation by SEB was markedly enhanced by dCB (Fig. 1E *left panel,* 80% to 90% activated and 7% to 23% highly activated, $IFN\gamma^+$) with aggregate data showing this benefit across the cohort (Fig. 1E *right panel,* paired t-test, $p<0.05$). The greater activation of post-transplant $CD8^+$ T-cells with checkpoint blockade is

consistent with the above described increased expression of checkpoints and increased sensitivity to checkpoint ligation. Additionally, neither pre- nor post-transplant $CD4^+$ T-cell activation significantly increased in response to dCB (Supp. Fig. 1E).

Taken together, these data suggest that – similar to canonical TCR-mediated activation – homeostatic activation is coupled to checkpoint-mediated homeostatic inhibition, but these can be effectively uncoupled by checkpoint blockade. Furthermore, these data suggest that dCB therapy may be significantly more (or exclusively) effective in the setting of T-cell transfer into lymphodepleted recipients than as a stand-alone therapy.

Homeostatic activation is coupled to homeostatic inhibition in a murine BMT model

To further determine the relationship between homeostatic activation and homeostatic inhibition we used a mouse model of syngeneic bone marrow and splenocyte transfer into lymphodepleted recipients. Mice received total body irradiation (TBI) recipients followed by cell transfer. Control recipients received syngeneic splenocytes without TBI (denoted “No Rx”). As observed in the patients, transfer into lymphodepleted recipients induced a phenotype indicating both homeostatic activation and homeostatic inhibition of the CD8+ T-cells (Fig. 2A and B). This was indicated by simultaneous upregulation of CD44, IL-2rβ and Ki-67 along with the inhibitory checkpoints PD1 and CTLA4. Because only $CD8^+$ T-cells evidenced transfer-induced homeostatic inhibition which could be reversed by dCB, we focused subsequent experiments on $CD8^+$ T-cells.

To determine functional effects of increased checkpoint expression on post-transplant T-cells, we assessed T-cell stimulation with concurrent ligation of PD1 or CTLA4 by plate-bound PD-L1 or CTLA4. As in our patients, the stimulation of post-BMT $CD8^+$ T-cells was enhanced as compared to the control cohort (Fig. 2C solid red vs. solid black). PD-L1 *only* inhibited $CD8^+$ T-cell cytokine production from BMT recipients (Fig. 2C solid red vs. checkered red). Similarly, activation of $CD8^+$ T-cells from BMT-treated mice was inhibited in the presence of CD80 (Fig. 2C *right panel*). Because PD1 induces Bim-mediated T-cell apoptosis [24], we assessed activation-induced cell death and observed that *only* post-BMT $CD8^+$ T-cells increased transition into early apoptosis in the presence of PD-L1 (Supp. Fig. 2A red solid vs. red checkered).

To test the ability of dCB to protect against homeostatic inhibition, mice were treated *in vivo* with dCB before (donor) and after (recipient) BMT – a combination approach we termed immunotransplant (IT). $CD8^+$ T-cells from IT recipients were not suppressed by exposure to PD-L1 and did not undergo apoptosis (Fig. 2C and Supp. Fig. 2A). *In vivo* dCB treatment also prevented suppression and partially restored activation in the presence of plate-bound CD80 (Fig. 2C *right panel*). These data suggest that checkpoint blockade before and after transfer into lymphodepleted recipients (IT) protects transferred $CD8^+$ T-cells from checkpoint-induced suppression. By uncoupling homeostatic inhibition from homeostatic activation, IT significantly increased the latter, as $CD8^+$ T-cells expressed higher levels of CD44, IL-2rβ and Ki-67 post-IT versus post-BMT (Supp. Fig. 2B). Thus, IT reveals the potential magnitude of uninhibited homeostatic activation.

Immunotransplant amplifies antigen-specific CD8 T-cell responses

Next, we determined whether IT would also enhance transfer of antigen-specific $CD8^+$ T-cell in to a lymphodepleted host. IT was performed using donor mice expressing a TCR specific for and congenic wildtype recipients. Wildtype mice were irradiated and subsequently received syngeneic GFP-specific T-cells, which recognize the immunodominant epitope of GFP ($GFP_{200–208}$) presented on H-2Kd [25, 26] either alone or with dCB. Recipient splenocytes were stimulated *in vitro* with GFP-expressing A20 lymphoma cells and assessed for IFNg production, shown to be necessary for tumor-cytolysis[27]. Antigen-specific $CD8^+$ T-cell activation was significantly greater in IT recipients than in mice receiving BMT or dCB alone (Fig. 2D). Mirroring the poor response to dCB seen in human NHL, dCB treatment in the absence of transfer into lymphodepleted mice ("dCB only") did not increase the constitutive- or Ag-specific activation of $CD8^+$ T-cells (Supp. Fig. 2B and Fig. 2D). These data establish that *in vivo*, dCB is especially beneficial to $CD8^+$ T-cells upon transfer to the lymphodepleted recipient, as seen *in vitro* with patient samples.

Immunotransplant induces tumor-specific immune responses, reverses T-cell exhaustion, and treats lymphoid and solid tumors

To determine whether the increased $CD8^+$ T-cell activation induced by IT could increase anti-tumor immunity, we developed an IT tumor model. A20 tumor-bearing donor mice were treated with dCB before splenocytes and bone marrow were harvested, splenocytes were transferred to A20 tumor-bearing TBI-treated syngeneic recipient mice, recipients received additional dCB after transfer. This therapeutic IT was compared to BMT – the same procedure without the dCB treatment – as well as 'dCB only' and 'No Rx' cohorts, which received no irradiation followed by bone marrow and splenocyte transfer.

IT therapy induced tumor regressions in the majority of recipients, whereas BMT or dCB alone induced only transient growth delay (Fig. 3A, *upper panel*). While dCB and BMT yielded durable remissions in 10% of recipients, IT significantly prolonged survival and yielded durable remissions in 40% (Fig. 3A, *lower panel*), i.e., without evidence of disease past 60 days. These data demonstrate that IT possesses additive or synergistic anti-tumor efficacy over its components, BMT and dCB, with kinetics suggesting that the effect is mediated by transferred immune cells.

To measure tumor-specific T-cell responses, recipient peripheral blood lymphocytes were stimulated *in vitro* with A20 lymphoma cells and assessed for activation. The proportion of tumor-specific $CD8^+$ T-cells (IFNγ-production in A20 co-culture) was significantly higher in IT-treated mice than in other cohorts and ~10-fold higher than in mice receiving dCB alone (Fig. 3B).

Tumors from each cohort were harvested and tumor-infiltrates assessed by immune-fluorescence, revealing marked, uniform infiltration of intratumoral $CD8^+$ T-cells in IT mice (Fig. 3C, *top panel*). To better understand the intratumoral immune repertoire, we performed mass cytometry (CyTOF) using a broad multiplex panel focused on T-cell activation state. Compared to dCB alone, both BMT and IT recipients demonstrated a ~6- to 7-fold increase

in the proportion of intratumoral $PD1^{hi}$ $CD8^{+}$ T-cells, a surrogate of tumor Ag-specific T-cells [28] (Fig. 3C, *bottom panel*).

While BMT and IT recipients had similar increases in intratumoral $PD1^{hi}CD8^{+}$ T-cells, there were marked differences in activation state between these cohorts. In BMT recipients, these T-cells had an exhausted phenotype, per their lower expression of CD122/IL-2Rβ [29] and higher expression of TIM-3 [30] (Fig. 3D, *right panel*), however their exhausted phenotype is distinct from conventional Ag/TCR-driven terminally exhausted T cells. These 'progenitor-like' T-bet ^{Hi} cells [31] are more responsive to checkpoint blockade [32].In IT recipients, we observed reversal of exhaustion, as $PD1^{hi}CD8^{+}$ T-cell proliferation (quantified by Ki-67) markedly increased, a correlate of anti-tumor efficacy in preclinical models and patients [33]. This T-cell subset in IT recipients also expressed significantly higher levels of T-bet, denoting residual potential for reinvigoration [34], proliferation [31], and salvage by checkpoint blockade [35].

The efficacy of IT was tested in additional lymphoid and solid tumor models. Mice bearing B16 melanoma (Fig. 3E *top panel*), KLN205 lung squamous cell carcinoma (Fig. 3E *middle panel*), or EL4 T-cell lymphoma tumors (Fig. 3E *bottom panel*) were treated as described above. IT induced regression and improved survival in all tumor models more effectively than dCB or BMT. In some models, such as lung carcinoma, IT yielded durable remissions of established tumors. As noted by others [36], even dCB therapy was minimally effective in all tumor models tested. Therefore, the significantly improved anti-tumor effect of IT in treating these established tumors appears to be greater than additive, suggesting a cooperative immune effect in combining dCB and T-cell transfer into lymphodepleted recipients.

Immunotransplant requires *double* checkpoint blockade, but does not increase toxicity

To determine whether the anti-tumor efficacy of IT requires blockade of both PD1 and CTLA4, cohorts were treated with BMT and IT as in Figure 3 with additional cohorts in which IT was performed using only anti-CTLA4 (IT [αCTLA4]) or anti-PD1 (IT [αPD1]). Mice that received the dCB and transfer (IT) showed significantly greater tumor regressions and improved survival than in either of the monotherapies (Supp. Fig. 3A). Furthermore, recipient peripheral blood lymphocytes from each cohort were stimulated *in vitro* with A20 lymphoma cells as described above. Recipients of dCB-treated IT had a 3- to 4-fold greater proportion of tumor-specific $CD8^{+}$ T-cells than recipients of IT with either single checkpoint blockade (Supp. Fig. 3B; IT compared to BMT or IT [αPD1]). These data show that dCB is necessary for the superior anti-tumor immunity observed with IT.

Checkpoint blockade therapy, especially dCB, can induce high-grade autoimmune toxicities in both patients and mice [37], including hepatoxicity, which has been amongst the most common of these [38]. Because IT increased anti-tumor immune responses, we assessed whether it also increased these toxicities. Serum from mice from each treatment cohort were assessed for liver enzyme levels. All three treatment cohorts (dCB, BMT, IT) showed mild enzyme elevations, though results in the IT cohort were similar to or better than in the dCB cohort and similar to described effects in combination immunotherapy studies (Supp. Fig. 3C). Likewise, while weight loss was seen in BMT and IT cohorts, results with IT were

similar to those with the BMT cohort (Supp. Fig. 3D) and similar to the effects described in syngeneic BMT studies [39] attributed to TBI.

Immunotransplant anti-tumor immunity is lymphodepletion-, CD8-, and IFNγ-dependent

To determine whether the primary role of TBI in the IT model is its lymphodepletive effect, and not its direct anti-tumor effects, treatments were repeated but with recipient tumor-challenge two days *after* irradiation, such that tumors were not exposed to TBI. In this format, IT recipients experienced transient tumor growth followed by regression, and ~80% experienced durable remissions (i.e., without evidence of disease past 60 days).By contrast, there was no significant survival prolongation with either BMT or dCB alone (Fig. 4A). Notably, the tumor regressions observed in IT recipients occurred in a time course consistent with the homeostatic proliferation/activation observed in earlier experiments (Fig. 2A and Supp. Fig. 2B). These data confirm that the IT anti-tumor effect is not a result of increased tumor radiosensitivity but primarily immune-mediated.

To determine cellular and molecular effectors of the anti-tumor immune response, IT recipients were depleted of $CD8^+$ T-cells (IT + αCD8), $CD4^+$ T-cells (IT + αCD4), or IFNγ (IT + αIFNγ) using depleting antibodies before transfer and continuously thereafter. IT anti-tumor immunity was diminished by $CD8^+$ T-cell and IFNγ depletion but not $CD4^+$ T-cell depletion (Fig. 4B). Because recipient lymphodepletion induced homeostatic activation of transferred $CD8^+$ T-cells (Fig. 2), we also confirmed that lymphodepletion was necessary for the observed anti-tumor effect. Mice were treated with IT, but recipient mice were not irradiated (IT+ 0Gy), which completely abrogated the anti-tumor effect (Fig. 4C; 'IT+0 Gy' orange line n.s. vs. 'No Rx' black line). The effectiveness of IT was also tested by substituting lymphodepleting chemotherapy for myeloablative TBI, using fludarabine and cyclophosphamide (Flu/Cy) as in clinical cellular therapies. There was no significant difference between Flu/Cy and TBI in IT (Fig. 4C; 'IT+ Flu/Cy' brown line n.s. vs. 'IT' purple line), suggesting that IT anti-tumor immunity may depend more on recipient lymphodepletion than on other effects of TBI, e.g., TLR agonism related to intestinal irradiation [40].

Due to the rapidity of tumor regressions noted in IT recipients (Fig. 3A), we hypothesized that the tumor-specific immune response required priming in the donor. To test this, donor mice with or without tumors were treated with dCB as described above prior to transfer. The anti-tumor immunity of IT was abolished by using tumor-free donors (Fig. 4C 'Donor No Tumor' blue line n.s. vs. 'No Rx' black line).

To determine the durability of the anti-tumor immune response, IT recipients that had cleared the tumor were re-challenged with A20 lymphoma or 4T1 breast cancer cells. Recipients were completely protected from A20 re-challenge (Fig. 4D; IT+ A20) but not from 4T1 (Fig. 4D; IT+ 4T1), indicative of a tumor-specific memory immune response. Taken together, these data show that the anti-tumor immunity of IT is durable, CD8- and IFNγ-dependent, and requires priming of a donor anti-tumor response and recipient lymphodepletion.

γ_c cytokine signaling is amplified by immunotransplant and necessary for anti-tumor immunity

As IT appears to modulate peripheral and intratumoral $CD8^+$ T-cell activation state, and because a broad range of cytokines regulate T-cell activation, we determined whether the increased homeostatic and tumor-specific activation might be cytokine-regulated. To evaluate differences in cytokine levels, serum concentration of 30 cytokines was assessed using a bead-based multiplex assay in mice of each treatment cohort. Of the 30 tested (Supp. Fig. 4A), the only cytokines that differed significantly between IT and other cohorts were the common gamma chain (γ_c) family members IL-2, IL-7 and IL-15, as well as TNFα (Supp. Fig 4B and Fig. 5A). Remarkably, the increase in serum γ_c concentrations in the IT cohort was greater than additive relative to the effects of dCB plus BMT. For example, the mean serum concentration of IL-2 was 4 pg/mL with dCB and 12.5 pg/mL with BMT but over 98 pg/mL in the IT cohort. Serum γ_c in patients receiving BMT are consistent with (or even several-fold higher than)[41] those observed in mice receiving BMT alone, suggesting that the our observations may translate well to the clinic.

IL-2, IL-7, and IL-15 induce signaling through a shared γ_c receptor and their respective alpha receptor components, with IL-2 and IL-15 sharing a third component IL-2Rβ/CD122. As such, we examined differences in the expression of γ_c receptor subunits by flow cytometry. IT and BMT were performed using congenic donors; in these experiments, the dCB and No Rx control cohorts were also recipient mice that received congenic splenocyte transfer but without TBI. IT treatment induced significantly higher expression of IL-15Rα, IL-2Rβ, and γ_c on transferred $CD8^+$ T-cells as compared to the other cohorts, but not IL-2Rα or IL-7Rα (Fig. 5B).

Next, we determined whether increased γ_c receptor subunit expression correlated with downstream signaling and increased sensitivity to receptor ligation. IL-2, IL-7, and IL-15 signal through the JAK-STAT pathway, primarily JAK1/3 and STAT5 [42]. Recipient splenocytes from each cohort were stimulated with recombinant IL-2, IL-7, and IL −15 *in vitro,* and signaling was measured per STAT5 phosphorylation. $CD8^+$ T-cells from IT recipients showed slightly higher basal levels of p-STAT5 and significantly higher levels of inducible p-STAT5 in response to all γ_c cytokines tested as compared to other cohorts (Fig. 5C). To determine whether increased γ_c cytokine signaling could potentiate TCR signaling, recipient splenocytes from each cohort were stimulated with suboptimal doses of α-CD3ε plus individual γ_c cytokines *in vitro* [43]. $CD8^+$ T-cells from IT-treated mice proliferated more robustly in response to IL-2 and IL-15 than in other cohorts (Fig. 5D). Of note, BMT recipients showed changes similar, though lesser, to IT mice in these metrics (Fig. 5B–D). These data suggest that IT not only increases γ_c cytokine production, but also γ_c subunit receptors on $CD8^+$ T-cells and sensitivity to receptor ligation.

To determine whether the increased JAK/STAT signaling in IT recipients potentiates physiologic TCR activation (as opposed to CD3ε ligation), IT was performed as previously, using GFP-reactive $CD8^+$ T-cell donors and *in vitro* stimulation with GFP-A20 lymphoma cells. As above, IT induced the greatest proportion of tumor-specific $CD8^+$ T-cells (Figs. 2D and Fig. 5E). However, when these $CD8^+$ T-cells were pretreated *in vitro* with the JAK3-specific inhibitor tofacitinib [44], the increased tumor-antigen-specific response was

abrogated (Fig. 5E). Conversely, when recipient splenocytes from each cohort were treated with a mix of IL-2, IL-7 and IL −15, antigen-specific cytokine production increased significantly for $CD8^+$ T-cells from the other cohort groups, and those from the BMT cohort became comparable to IT (Fig. 5E). These results suggest that the amplified tumor-specific $CD8^+$ T-cell responses observed with IT depend upon γ_c cytokine signaling.

To determine the importance of IL-7 or IL-15 signaling in enhancing the function of anti-tumor T-cells induced by IT, IL-7Rα(−/−) or IL-15Rα(−/−) donor mice (and wildtype recipients) were used for IT, as previously described. If donor splenocytes lacked IL-7Rα or IL-15Rα, IT anti-tumor immunity was greatly reduced or abolished (Fig. 5F). These data confirm that γ_c cytokine signaling is critical in augmenting the anti-tumor immune response observed with IT.

BMT increases γ_c receptor and signaling on donor T-cells in lymphoma patients

To determine if molecular mechanisms critical to the anti-tumor effect of the preclinical IT model could be observed in patients, we measured γ_c receptor expression and function in our autologous BMT patient cohort (Fig. 5B–D). Common gamma chain receptor expression was assessed by flow cytometry on pre- and post-transplant PBMCs. Similar to BMT-treated mice, post-transplant $CD8^+$ T-cells expressed higher levels of IL-15Rα, IL-2Rβ, and γ_c receptors but not IL-2Rα or IL-7Rα (Fig. 6A).

Next, pre- and post-transplant PBMCs were stimulated with *in vitro* IL-2, IL-7, and IL-15, and p-STAT5 was measured by flow cytometry. As seen in mice, post-transplant $CD8^+$ T-cells were more sensitive and responsive to γ_c cytokines, inducing significantly increased levels of p-STAT5 (Fig. 6B). Furthermore, post-transplant $CD8^+$ T-cells showed greater proliferation in response to IL-2 and IL-15 stimulation, with a similar trend for IL-7 (Fig. 6C). These data confirm similar changes in γ_c cytokine and responses in patients and mice treated with BMT.

Given our initial finding of increased checkpoint molecules on post-BMT patient $CD8^+$ T-cells, we returned to more broadly assess their activating and inhibitory phenotype by mass cytometry. We observed that homeostatic inhibition may extend beyond PD1/CTLA4 as marked upregulation of other $CD8^+$ T-cell inhibitory checkpoints (e.g., TIGIT, TIM3, LAG3, CD38) were also observed post-BMT (Fig. 6D *left panel*). Though patient and murine T-cell panels differed, overall, similar phenotypic changes were seen, with BMT inducing upregulation of TIGIT, and CXCR3 and downregulation of CD103 on both patient and murine T-cells (Fig. 6D *right panel*). Thus, suggesting the similarities between our mouse model and patients if generally conserved.

BMT and γ_c cytokines induce JAK3-dependent homeostatic activation and inhibition

To determine if the upregulation of PD1 and CTLA4 that we observed is γ_c cytokine-dependent, we took advantage of genetic knockouts of the cytokine receptors. When splenocytes from IL-7Rα (−/−) and IL-15Rα (−/−) mice were transferred into TBI-treated wild type recipient mice upregulation of PD1 and CTLA4 was significantly reduced on CD8+ T-cells post-transplant (Fig. 7A). Furthermore, disruption of these receptors also abrogated $CD8^+$ T-cell homeostatic proliferation and activation (Fig. 7B), suggesting that

homeostatic activation as well as the concomitant homeostatic inhibition are γ_c cytokine-dependent.

Next we assessed mechanisms of this novel finding further by using γ_c cytokine-treated T-cells as a surrogate for lymphopenia-exposed T-cells. Using healthy donor human PBMCs or naïve mouse splenocytes, we confirmed that *in vitro* treatment with IL-2, IL-7 or IL-15 induces PD1 on human and mouse $CD8^+$ T-cells (Fig. 7C), while IL-2 and IL-15 also induced CTLA4 expression on $CD8^+$ T-cells (Fig. 7C). Additionally, IL-2 and IL-15 induced the homeostatic activation markers Ki-67, IL-2rβ, and CD44 on human $CD8^+$ T-cells, while all three γ_c cytokines induced Ki-67 and IL-2rβ on mouse $CD8^+$ T-cells (Supp. Fig. 5A).

Signaling of γ_c cytokines are mediated primarily through JAK1/3, and it has been shown that JAK3 inhibition is sufficient to abrogate downstream STAT5-signaling in immune cell subsets [45]. When γ_c cytokine-treated healthy human PBMCs or naïve mouse splenocytes were pre-incubated with the JAK3 inhibitor tofactinib, γ_c cytokine-induced PD1 and CTLA4 upregulation were significantly inhibited (Fig. 7D), as was homoeostatic activation (Supp. Fig. 5B).

To determine whether the PD1 and CTLA4 induced on healthy human PBMCs by IL-15 were functional, the cells were activated by ligating CD3 and CD28 with or without plate-bound PD-L1. The γ_c cytokine-induced $PD1^{hi}$ $CD8^+$T-cells were more apoptotic in the presence of PD-L1 (Supp. Fig 5C). Similarly, in the presence of PD-L1 or CD80, the high PD1- and CTLA4-expressing $CD8^+$ T-cells were less activated (Supp. Fig. 5D). Taken together, these data suggest that transfer-induced homeostatic activation and homeostatic inhibition are largely dependent upon – and regulated by – γ_c cytokine signaling.

Discussion

Homeostatic activation of T-cells transferred into the lymphodepleted recipient is routinely exploited in the lab and the clinic to amplify the anti-tumor efficacy of T-cell therapies [10–13]; however, the concurrent homeostatic inhibition has not been well recognized or addressed. Here we demonstrate that transfer into a lymphodepleted recipient induces functional PD1 and CTLA4 (amongst numerous checkpoint molecules) in both patient and murine CD8+ T-cells. This homeostatic inhibition can be reversed with dCB to reveal the underlying magnitude of homeostatic T-cell activation per improved T-cell proliferation, tumor-specific IFNγ production, and tumoricidal activity. Homeostatic activation combined with dCB yielded a synergistic increase in patient and murine T-cell function. DCB alone did *not* increase IFNγ production upon TCR ligation but did so only in the context of homeostatic activation. These data predict the *in vivo* results in lymphoma, melanoma and lung cancer models, in which dCB yielded no significant benefit but immunotransplant induced tumor regressions and improved survival.

Homeostatic inhibition is –at least partly– regulated by γ_c cytokines and thereby mechanistically coupled to homeostatic activation [19, 20], i.e., IL-7R/15R expression on donor T-cells are required for PD1 and CTLA4 upregulation and for the anti-tumor effects of

IT. These data are consistent with prior results showing that IL-7/15 increase post lymphodepletion [46] and mediate checkpoint blockade therapy anti-tumor efficacy [47].

While it is well established that T-cell activation induces T-cell inhibitory signals, prior to this work, the specific mechanisms of how homeostatic activation induces inhibitory signals were not well understood. Mechanistic coupling by γ_c cytokine signaling could not be presupposed. Because TBI also modulates transferred T-cells by IL-7/15-*independent* mechanisms (e.g., microbial activation of enteric TLR and host DC-produced IL-12)[48], it might have been the case that homeostatic activation is mediated by γ_c cytokines and homeostatic inhibition mediated by TLR agonism. Conversely, uncoupling of these processes by PD1 and CTLA4 blockade could not be presupposed; numerous checkpoints are upregulated post-BMT including TIGIT, TIM3, LAG3 and CD38 (Fig. 6D), any of which might mediate T-cell inhibition. While PD1/CTLA4 blockade uncouples the competing effects of IL-7/15 on transferred T-cells, blocking these other checkpoints *might* further reverse homeostatic inhibition, one avenue of ongoing investigation.

Downstream, γ_c receptors signal through JAK 1/3 and STAT5, known mediators of T-cell anti-tumor efficacy [49]. While IL-7/15 *can* signal through JAK1 [50], notably, both the activating (Fig. 5E) and inhibitory (Fig. 7D) effects of γ_c cytokine signaling appeared to be JAK3-dependent, another level of mechanistic coupling. Further downstream, because JAK3 signals largely through STAT5 [51], it is noteworthy that both PD1 and CTLA4 signaling have been implicated in STAT5 inhibition and sequestration [52, 53]. Reversal of such sequestration is a potential mechanism for enhanced STAT5 signaling in IT (vs. BMT) recipients. We observed increased basal STAT5 phosphorylation in the T-cells of IT recipients as well as increased γ_c cytokine sensitivity, indicating the interaction of checkpoint signaling with the JAK/STAT pathway. STAT5 regulates expression of Eomes and T-bet in T-cells and thereby reversal of exhaustion [54] and cytotoxic function [55]. It is likely that atypical 'progenitor-like' T- bet^{hi} exhausted cells observed post-BMT are the product of a mechanistically distinct exhaustion downstream from different means of NFAT activation. In contrast to TCR-mediated exhaustion which results from calcineurin-*dependent* NFAT signaling [56], instead common γ-chain cytokines induce calcineurin-*independent* NFAT by means of a novel Y371 phosphorylation [57, 58]. The favorable T-bet^{hi} Eomes^{lo} phenotype [55]and markedly increased proliferative rate of intratumoral T-cells in IT recipients suggests that, ultimately, using dCB to uncouple homeostatic inhibition from activation potentiates anti-tumor T-cell responses.

We propose a model (Supp. Fig. 5E) whereby, on transfer to BMT recipients, IL-7 and IL-15 activate T-cells, but also induces mediators (e.g. NFAT) that increase the transcription of PD1, CTLA4, and other checkpoints. PD1 and CTLA4 ligation promotes SHP2 inhibitory signaling. The resulting inhibitory signals prevent maximal homeostatic activation. Though blocking these γ_c cytokines would obviate both their activating and inhibitory effects, blocking PD1/CTLA4 further downstream uncouples these effects. Checkpoint blockade in this setting (immunotransplant), relieves inhibition of *both* TCR signaling (e.g. decreasing SHP2-activity) as well as JAK/STAT signaling (e.g. decreasing STAT5 sequestration). The resulting JAK/STAT signaling likely induces T-bet[59] and thereby homeostatic activation markers (IL- 2rβ, CD44), cytokines (IL-2, IFNγ) production, and anti-tumor effects.

Our results connect prior preclinical and clinical observations. Kinter et al. observed increased T-cell PD1 expression upon *in vitro* γ_c cytokine exposure [60], while Fortner et al. noted increased PD1 and LAG3 transcripts in murine T-cells after transfer into lymphocyte deficient mice[61]; these results were confirmed and expanded upon by our studies, but these studies did not determine the potential of checkpoint blockade in these settings. Kearl et al. used an approach comparable to our IT model but without CTLA4 blockade, myeloablative TBI, donor priming or T-cell transfer. Still, Kearl et al.'s data demonstrated significant anti-tumor effects, though their therapy insufficient for benefit in B16 or EL4 models [62], both of which were effectively treated in our IT model. While, Jing *et al.* included TBI in a dCB-based regimen, they did not evaluate the necessity of TBI or endeavor to understand the mechanisms that underlie the benefits of combining TBI and checkpoint blockade [63]. Finally, Vu et al. observed increased expression of *costimulatory* molecules – OX40, ICOS, and CD137 – on homeostatically activated T-cells [64], complementing our observations of increased checkpoint molecule expression after homeostatic activation. Indeed, the basic concepts underlying our observations are not entirely novel, increased checkpoint expression post-BMT has been previously observed [65]and early studies of checkpoint blockade in this context have been initiated [66] (NCT02362997, NCT02771197, NCT02681302, NCT02331368). The observations herein add mechanistic insight and additional data on the activation state of tumor-specific T cells induced by each component (dCB and BMT) of the combined therapy.

The patient and preclinical data predict that immunotransplant may provide clinical benefit in patients with aggressive lymphoma, despite the limited efficacy of dCB in these patients [3]; currently being evaluated in an ongoing trial (NCT03305445). Using IT to enhance the efficacy of dCB could be broadly significant; dCB is a standard therapy for melanoma, renal cell cancer, and subsets of colorectal cancer [67] and lung cancer [38] and in numerous ongoing trials for other cancers. Even for settings in which dCB proves ineffective, our data suggest that dCB efficacy may be 'rescued' by IT. Conversely, as homeostatic activation might improve dCB therapy, the addition of checkpoint blockade may improve T-cell therapies already exploiting lymphodepletion, such as CAR-T therapy. Anecdotal evidence of that approach is promising [68], and larger studies are underway (NCT02926833).

Despite the importance of γ_c cytokines for T-cell activation, their development as cancer therapies has been elusive. Recent improvements in γ_c cytokine formulation and dosing [69] have yielded promising preliminary results, prompting combination trials with checkpoint blockade [69]. Our IT approach, similarly, provides transferred T-cells with increased access to (endogenous) γ_c cytokines. A notable distinction is that recombinant γ_c cytokine therapy induces tachyphylaxis with continued exposure [70, 71], whereas IT approach actually increases γ_c cytokine receptor expression and signaling. Regardless of the optimal approach for providing γ_c cytokines clinically, assessing homeostatic inhibition with these therapies will be important. Rather than presumptively combining all such therapies with PD1 blockade, the specific inhibitory checkpoints elicited by *each* therapy should be determined, e.g., one γ_c cytokine therapy may increase T-cell expression of CTLA4 and LAG-3 while another increases PD1 and TIGIT.

Addressing homeostatic inhibition is not limited to the blockade of PD1 and CTLA4. Our data revealed significant increases in CD8 T-cell expression of TIGIT, TIM3, LAG3, and CD38 post-BMT; all of which are currently being targeted in clinical trials. Further preclinical study of these and other checkpoint targets could expand our understanding of homeostatic inhibition and could translate into novel rational combinatorial approaches for patients, particularly those with tumor types in which immunotherapy has yet to offer significant benefit.

Methods

Ethical Compliance

Written Informed Consent was obtained from patients in accordance with Declaration of Helsinki and Protocols were approved by Mount Sinai Institutional Review Board.

Protocols for the treatment of patients, as well as human sample collection and analysis, were approved by the Mount Sinai Institutional Review Board, and written informed consent was obtained from all patients. All experiments including human specimens were performed in compliance with the relevant ethical regulations

Cell lines

A20, B16, EL4, and KLN205 were purchased from ATCC. Cells were cultured as described by ATCC, except EL4 were cultured in complete RPMI-1640 media plus 1mM sodium pyruvate. Heat inactivated FBS was purchased from Gemini Bioproducts. All cells were tested and confirmed mycoplasma negative with Universal Mycoplasma Detection Kit (ATCC) before in vitro culturing and again before in vivo injection. A20 cells were tested in 2014 and 2016, B16 in 2014, KLN205 in 2017, EL4 in 2017. No cell authentication was performed. Cells were cultured at 37 °C in 5% CO_2. Cells were cultured 7 days after un-thawing before in vitro and in vivo.

Mice

Six- to 10-week-old male BALB/c, C57BL/6, DB2/A, B6129SF2/J; and breeding pairs of B6.129S7-*Il7r*^{tm1Imx}/J (IL-7rα KO) and B6; 129X1-*Il15ra*^{tm1Ama}/J (IL-15rα KO) mice were ordered from Jackson Laboratories. Mice were maintained in barrier conditions. All experiments involving live mice were performed in compliance with ethical regulations approved by the Institutional Animal Care and Use Committee of the Icahn School of Medicine at Mount Sinai (New York, NY).

Immunotransplant

Seven- to nine-week-old donor and recipient male BALB/c mice were inoculated with 1×10^6 A20 cells subcutaneously in the right hind flank. One week after tumor inoculation, the donor was treated with 100μg of anti-PD1 (RMP1–4; BioXCell) and anti-CTLA4 (9H10; BioXcell) per mouse 3 times 3 days apart. Three days after the final injection, recipient mice were irradiated with 900 cGy of TBI in a Rad Source RS-2000 Biological System unit. The spleens and bone marrow of donor mice were harvested. Irradiated recipients were injected intravenously with 0.3 mL in HBSS in the tail vein admixed with splenocytes and bone

marrow cells. Splenocyte dose was one spleen per recipient and 5×10^6 bone marrow cells per mouse.

Beginning the day of ablative therapy and for two weeks after, drinking water was supplemented with 1 mg/mL neomycin and 1000U/ml Polymyxin Sulfate B (Sigma-Aldrich) for gut decontamination.

Immunotransplant was tested in other tumor models as described, with the following modifications:

5×10^5 B16 cells were inoculated subcutaneously in the right hind flank of male C57BL/6 donor and recipient mice. Recipient mice were treated 6 times with 100μg of anti-PD1 and CTLA4.

2×10^5 EL4 cells were inoculated subcutaneously in the right hind flank of the male C57BL/6 donor and recipient mice. Recipient mice received 600 cGy of TBI.

Recipient mice were treated 6 times with 100μg of anti-PD1 and CTLA4.

1×10^6 KLN205 cells were inoculated subcutaneously in the right hind flank of the male C57BL/6 donor and recipient mice.

5×10^5 B16 cells were inoculated subcutaneously in the right hind flank of the male IL-7Rα KO donor and male C57BL/6 recipient mice. Splenocyte dose was five IL-7Rα KO donor spleen per one C57BL/6 WT recipient and 5×10^6 bone marrow (BM) cells per mouse. 2×10^5 EL4 cells were injected subcutaneously in the right hind flank of the female IL-15Rα KO donor and female B6129SF2/J WT recipient mice. Recipient mice were irradiated with 600 cGy of TBI. Splenocyte dose was two IL-15Rα KO donor spleen per one B6129SF2/J WT recipient and 5×10^6 bone marrow (BM) cells per mouse.

Antibodies

The following antibodies were used during this study:

Human—PD1 (EH12.1), IL-2Rα /CD25 (M-A251), CD8 (RPA-T8), CD3 (SK7), CD4 (RPA-T4), CTLA4 (BNI3), γ_c (TUGh4), IL-2Rβ (TU27), IL-7Rα (A019D5), IL-15Rα (JM7A4), Ki67 (KI67 Biolegend), CD44 (BT18), IFNγ (4S.B3), TNFα (Mab11), pSTAT5 (pY694; Clone 47)

Mouse—B220 (RA3–6B2), CTLA4 (UC10–4B9), CD127 (SB/1999), IFNγ (XMG1.2), CD69 (H1.2F3), TCRβ (H57–597), IL-2 (JES6–5H4), TNFα (MP6-XT22), CD45.1 (A20), CD45.2 (104), IL-2Rα/CD25 (PC61), CD3 (145-SC11), CD8 (53–6.7), CD4 (RM4–5), PD1 (J43), CD8β (eBioH35–17.2), pSTAT5 (pY694; Clone 47), $H2K^d$ HALSTQSAL pentamer (Proimmune), IL-2Rβ (TM-Beta 1), IL-15Rα (DNT1Ra), Thy1.1 (OX-7), Thy1.2 (53.21)

Phospho-flow cytometry

Patient PBMCs were thawed and incubated for 30 minutes at 37 °C then cultured with recombinant human carrier-free IL2 (R&D), IL-7 and IL-15 (both PrepoTech) with Fixable Viability Stain for 15 minutes at 37 °C.

Murine splenocyte single cell suspensions were cultured with 100ng recombinant carrier free of mouse IL-2, IL-7 and IL-15 (Gemini Bioproducts) with BG Horizon Fixable Viability Stain (BD Biosciences) for 20 minutes at 37 °C.

Signaling was stopped by IC Fixation Buffer (Thermo-Fisher). Extracellular and nuclear staining was performed as described in BD Perm IV manual (BD Biosciences).

Plate-bound activation assays

Human—Flat-bottom 96-well plates were coated with the described amounts of anti-CD3 (OTK3; eBioscience) and human recombinant PD-L1-Fc (Biolegend), CD80-Fc (Biolegend), or IgG1-Fc (Sino Biological) diluted in PBS overnight at 4 °C. Mixture was aspirated, and PBMCs were cultured with soluble anti-CD28 (CD28.2; BD Biosciences) for the described amounts of time.

Mouse—Single-cell suspensions of splenocytes were CD8 T-cell-enriched with MagniSort mouse CD8 T-cell enrichment kit (Invitrogen). Flat-bottom 96-well plates were coated with the described amounts of anti-CD3ε (145–2C11; BD Biosciences) and mouse recombinant PD-L1-Fc (Biolegend), CD80-Fc (Biolegend), or IgG1-Fc (Sino Biological) diluted in PBS overnight at 4 °C. The mixture was aspirated, and CD8 T-cells were cultured with soluble anti-CD28 (37.51; BD Biosciences) for the described amounts of time.

SEB assay

PBMCs were cultured with 10μg of ipilimumab and nivolumab for 48 hours. Cells were washed and replenished with fresh ipilimumab, nivolumab and media. Then, they were co-cultured with 100ng of SEB (Toxin Technology) for another 72 hours.

Depletion studies

Immunotransplant-treated recipient mice were depleted of CD8 T-cells using with 250μg anti-CD8 (2.43), CD4 T-cells using anti-CD4 (GK1.5). IFNγ using 500μg of anti-IFNγ (R4–6A2). Recipient mice were treated with antibody three days before transplantation, the day of transplantation, every three days until the study's completion.

Detection of tumor-reactive T-cells

Mice were retro-orbitally bled, and blood was anticoagulated with 2 mM EDTA in PBS, then diluted 1:1 with Dextran T500 (Pharmacosmos) 2% in PBS and incubated at 37 °C for 45 minutes to precipitate red cells. PBMCs were then co-cultured with 5×10^5 irradiated A20 cells for 48 hours with 1μg mouse anti-CD28 and in the presence of brefeldin A (Invitrogen) for the last 5 hours at 37 °C.

Detection of GFP-reactive T-cells

GFP-specific donor mice (B10.D2 mouse strain background) were bred with BALB/c mice. F1 pups were tested by PCR for recombined alpha and beta chains in the TCR and confirmed to be GFP-reactive. F1 mice were treated with 100μg anti-CTLA4 and anti-PD1 3 times 3 days apart. Splenocytes were intravenously injected into congenic, irradiated F1 B10.D2-BALB/c mice. Recipient mice were also treated with 100μg anti-CTLA4 and anti-PD1 3 times 3 days apart. Recipient mice were harvested 7 days post-transfer. At a ratio of 20:1, splenocytes were cultured with GFP – overexpressing A20 *in vitro* for 24 hours, with the last 8 hours in the presence of brefeldin A.

Congenic mouse transfer

Donor BALB/c mice were treated with 100μg anti-CTLA4 and anti-PD1 three times three days apart. Three days after the final treatment, donor splenocytes were harvested and intravenously injected into congenic, irradiated BALB/C recipient mice. Recipient mice received one treatment of 100μg anti-CTLA4 and anti-PD1. Three days post transfer, splenocytes of recipient mice were harvested.

Immunofluorescent Microscopy

Tumors were excised after 14 days and placed in 10% formalin (Fisher Scientific) at room temperature overnight. Tumors were submerged in 15% sucrose in PBS for 6 hours, then 30% sucrose in PBS for 6 hours. Tumors were embedded in a base mold (Fisher Scientific) filled with filled with OCT (Fisher Scientific). Cryosections were cut at a thickness of 10μm using a Leica cryostat and mounted on SuperFrost Plus slides (Fisher Scientific) and permeabilized for 20 minutes in 0.5% Triton X-100 in PBS at room temperature. The primary antibodies stained.The sample slides were counterstained with 4’6’-diamidino-2-phenilindole (DAPI) and cover-slipped with Prolong Gold Anti-fade Reagent (Life Technologies). Imaging was performed using a Zeiss LSM780 confocal microscope. Images were collected using Zeiss ZEN software.

Time-of-flight mass cytometry (CyTOF)

Tumor cell suspensions were then depleted of tumor cells by magnetic separation using CD19-nanobeads according to the manufacturer’s protocol (Mojosort, Biolegend).

Viability staining was performed using Cell-ID™ Intercalator-103Rh (Fluidigm). Barcoding was performed by staining each sample with a unique combination of up to 4 different metal conjugations of a monoclonal antibody against CD45. Samples were then combined for further staining. Surface staining was performed in staining buffer containing FcX (Biolegend) and metal-conjugated antibodies. For intracellular staining, cells were incubated in Cytofix/Cytoperm (BD Biosciences) and stained with metal-conjugated antibodies in Perm/Wash buffer with heparin. Cells were washed and stained with Cell-ID™ Intercalator-Ir (Fluidigm) to label all nucleated cells. Acquisition was performed on a CyTOF2 cytometer, and data were analyzed with Cytobank.

Data availability

The datasets supporting the findings presented in this study are available from the corresponding author upon reasonable request. All requests for data and materials will be promptly reviewed by the Icahn School of Medicine at Mount Sinai to verify whether the request is subject to any intellectual property or confidentiality obligations. Any data that can be shared will be released via a Material Transfer Agreement.

Supplementary Material

Refer to Web version on PubMed Central for supplementary material.

Acknowledgements

We thank Dr. Peter Heeger for critically reading and editing this manuscript. We also thank the core facilities of Flow Cytometry CORE, the Center for Comparative Medicine and Surgery, and the Human Immune Monitoring Center at Ichan School of Medicine Mount Sinai.

Research reported in this publication was supported by the Tisch Cancer Institute through the National Cancer Institute Cancer Center Support Grant (P30 CA196521).

N.L.M. is funded by the NIH T32 Transplant 5T32AI078892 and T32 Immunology 5T32AI007605 grants.

B.D.B. is funded by a grant from the Cancer Research Institute and by NIH R21HD091461.

M.M. is funded by NIH R01 CA154947 and R01 CA190400.

J.D.B. is funded by a grant from Damon Runyon Cancer Research Foundation and by NIH 5R00CA140728.

References

1. Philip T, et al., Autologous bone marrow transplantation as compared with salvage chemotherapy in relapses of chemotherapy-sensitive non-Hodgkin's lymphoma. N Engl J Med, 1995 333(23): p. 1540–5. [PubMed: 7477169]
2. Ansell SM, et al., PD-1 blockade with nivolumab in relapsed or refractory Hodgkin's lymphoma. N Engl J Med, 2015 372(4): p. 311–9. [PubMed: 25482239]
3. Ansell S, Gutierrez ME, Shipp MA, Gladstone D, Moskowitz A, Borello I, Popa-Mckiver M, Farsaci B, Zhu L, Lesokhin AM, & Armand P, *A* Phase 1 Study of Nivolumab in Combination with Ipilimumab for Relapsed or Refractory Hematologic Malignancies (CheckMate 039). Blood, 2016 128(183).
4. Cerami E, et al., The cBio cancer genomics portal: an open platform for exploring multidimensional cancer genomics data. Cancer Discov, 2012 2(5): p. 401–4. [PubMed: 22588877]
5. Hammerich L, et al., Systemic clinical tumor regressions and potentiation of PD1 blockade with in situ vaccination. Nat Med, 2019 25(5): p. 814–824. [PubMed: 30962585]
6. Baker K, et al., Neonatal Fc receptor expression in dendritic cells mediates protective immunity against colorectal cancer. Immunity, 2013 39(6): p. 1095–107. [PubMed: 24290911]
7. Courtney AH, Lo WL, and Weiss A, TCR Signaling: Mechanisms of Initiation and Propagation. Trends Biochem Sci, 2018 43(2): p. 108–123. [PubMed: 29269020]
8. Surh CD and Sprent J, Homeostasis of naive and memory T cells. Immunity, 2008 29(6): p. 848–62. [PubMed: 19100699]
9. Larbi A and Fulop T, From "truly naive" to "exhausted senescent" T cells: when markers predict functionality. Cytometry A, 2014 85(1): p. 25–35. [PubMed: 24124072]
10. Neelapu SS, et al., Axicabtagene Ciloleucel CAR T-Cell Therapy in Refractory Large B-Cell Lymphoma. N Engl J Med, 2017 377(26): p. 2531–2544. [PubMed: 29226797]

11. Tran E, et al., T-Cell Transfer Therapy Targeting Mutant KRAS in Cancer. N Engl J Med, 2016 375(23): p. 2255–2262. [PubMed: 27959684]
12. Morgan RA, et al., Cancer regression in patients after transfer of genetically engineered lymphocytes. Science, 2006 314(5796): p. 126–9. [PubMed: 16946036]
13. Blaise D and Castagna L, Do different conditioning regimens really make a difference? Hematology Am Soc Hematol Educ Program, 2012. 2012: p. 237–45.
14. Hamilton SE, et al., The generation of protective memory-like CD8+ T cells during homeostatic proliferation requires CD4+ T cells. Nat Immunol, 2006 7(5): p. 475–81. [PubMed: 16604076]
15. Min B, et al., Spontaneous and homeostatic proliferation of CD4 T cells are regulated by different mechanisms. J Immunol, 2005 174(10): p. 6039–44. [PubMed: 15879097]
16. Murali-Krishna K and Ahmed R, Cutting edge: naive T cells masquerading as memory cells. J Immunol, 2000 165(4): p. 1733–7. [PubMed: 10925249]
17. Goldrath AW and Bevan MJ, Low-affinity ligands for the TCR drive proliferation of mature CD8+ T cells in lymphopenic hosts. Immunity, 1999 11(2): p. 183–90. [PubMed: 10485653]
18. Lin L, et al., Ex vivo conditioning with IL-12 protects tumor-infiltrating CD8(+) T cells from negative regulation by local IFN-gamma. Cancer Immunol Immunother, 2019 68(3): p. 395–405. [PubMed: 30552459]
19. Tan JT, et al., Interleukin (IL)-15 and IL-7 jointly regulate homeostatic proliferation of memory phenotype CD8+ cells but are not required for memory phenotype CD4+ cells. J Exp Med, 2002 195(12): p. 1523–32. [PubMed: 12070280]
20. Gattinoni L, et al., Removal of homeostatic cytokine sinks by lymphodepletion enhances the efficacy of adoptively transferred tumor-specific CD8+ T cells. J Exp Med, 2005 202(7): p. 907–12. [PubMed: 16203864]
21. Cho BK, et al., Homeostasis-stimulated proliferation drives naive T cells to differentiate directly into memory T cells. J Exp Med, 2000 192(4): p. 549–56. [PubMed: 10952724]
22. Muraille E, et al., B7.2 provides co-stimulatory functions in vivo in response to staphylococcal enterotoxin B. Eur J Immunol, 1995 25(7): p. 2111–4. [PubMed: 7542606]
23. Deshpande P, et al., IL-7- and IL-15-mediated TCR sensitization enables T cell responses to self-antigens. J Immunol, 2013 190(4): p. 1416–23. [PubMed: 23325887]
24. Ishida Y, et al., Induced expression of PD-1, a novel member of the immunoglobulin gene superfamily, upon programmed cell death. EMBO J, 1992 11(11): p. 3887–95. [PubMed: 1396582]
25. Agudo J, et al., GFP-specific CD8 T cells enable targeted cell depletion and visualization of T-cell interactions. Nat Biotechnol, 2015 33(12): p. 1287–1292. [PubMed: 26524661]
26. Agudo J, et al., Quiescent Tissue Stem Cells Evade Immune Surveillance. Immunity, 2018 48(2): p. 271–285 e5. [PubMed: 29466757]
27. Wroblewska A, et al., Protein Barcodes Enable High-Dimensional Single-Cell CRISPR Screens. Cell, 2018 175(4): p. 1141–1155 e16. [PubMed: 30343902]
28. Ahmadzadeh M, et al., Tumor antigen-specific CD8 T cells infiltrating the tumor express high levels of PD-1 and are functionally impaired. Blood, 2009 114(8): p. 1537–44. [PubMed: 19423728]
29. Intlekofer AM, et al., Effector and memory CD8+ T cell fate coupled by T-bet and eomesodermin. Nat Immunol, 2005 6(12): p. 1236–44. [PubMed: 16273099]
30. Blackburn SD, et al., Coregulation of CD8+ T cell exhaustion by multiple inhibitory receptors during chronic viral infection. Nat Immunol, 2009 10(1): p. 29–37. [PubMed: 19043418]
31. Paley MA, et al., Progenitor and terminal subsets of CD8+ T cells cooperate to contain chronic viral infection. Science, 2012 338(6111): p. 1220–5. [PubMed: 23197535]
32. Blackburn SD, et al., Selective expansion of a subset of exhausted CD8 T cells by alphaPD-L1 blockade. Proc Natl Acad Sci U S A, 2008 105(39): p. 15016–21. [PubMed: 18809920]
33. Kamphorst AO, et al., Proliferation of PD-1+ CD8 T cells in peripheral blood after PD-1-targeted therapy in lung cancer patients. Proc Natl Acad Sci U S A, 2017 114(19): p. 4993–4998. [PubMed: 28446615]

34. Huang AC, et al., T-cell invigoration to tumour burden ratio associated with anti-PD-1 response. Nature, 2017 545(7652): p. 60–65. [PubMed: 28397821]
35. Kao C, et al., Transcription factor T-bet represses expression of the inhibitory receptor PD-1 and sustains virus-specific CD8+ T cell responses during chronic infection. Nat Immunol, 2011 12(7): p. 663–71. [PubMed: 21623380]
36. Dai M, et al., Curing mice with large tumors by locally delivering combinations of immunomodulatory antibodies. Clin Cancer Res, 2015 21(5): p. 1127–38. [PubMed: 25142145]
37. Michot JM, et al., Immune-related adverse events with immune checkpoint blockade: a comprehensive review. Eur J Cancer, 2016 54: p. 139–148. [PubMed: 26765102]
38. Hellmann MD, et al., Nivolumab plus Ipilimumab in Lung Cancer with a High Tumor Mutational Burden. N Engl J Med, 2018 378(22): p. 2093–2104. [PubMed: 29658845]
39. Duran-Struuck R and Dysko RC, Principles of bone marrow transplantation (BMT): providing optimal veterinary and husbandry care to irradiated mice in BMT studies. J Am Assoc Lab Anim Sci, 2009 48(1): p. 11–22. [PubMed: 19245745]
40. Scholch S, et al., Radiotherapy combined with TLR7/8 activation induces strong immune responses against gastrointestinal tumors. Oncotarget, 2015 6(7): p. 4663–76. [PubMed: 25609199]
41. Thiant S, et al., Plasma levels of IL-7 and IL-15 in the first month after myeloablative BMT are predictive biomarkers of both acute GVHD and relapse. Bone Marrow Transplant, 2010 45(10): p. 1546–52. [PubMed: 20190846]
42. Rochman Y, Spolski R, and Leonard WJ, New insights into the regulation of T cells by gamma(c) family cytokines. Nat Rev Immunol, 2009 9(7): p. 480–90. [PubMed: 19543225]
43. Cho JH, et al., T cell receptor-dependent regulation of lipid rafts controls naive CD8+ T cell homeostasis. Immunity, 2010 32(2): p. 214–26. [PubMed: 20137986]
44. Changelian PS, et al., Prevention of organ allograft rejection by a specific Janus kinase 3 inhibitor. Science, 2003 302(5646): p. 875–8. [PubMed: 14593182]
45. Telliez JB, et al., Discovery of a JAK3-Selective Inhibitor: Functional Differentiation of JAK3-Selective Inhibition over pan-JAK or JAK1-Selective Inhibition. ACS Chem Biol, 2016 11(12): p. 3442–3451. [PubMed: 27791347]
46. Bolotin E, et al., Serum levels of IL-7 in bone marrow transplant recipients: relationship to clinical characteristics and lymphocyte count. Bone Marrow Transplant, 1999 23(8): p. 783–8. [PubMed: 10231140]
47. Shi LZ, et al., Interdependent IL-7 and IFN-gamma signalling in T-cell controls tumour eradication by combined alpha-CTLA-4+alpha-PD-1 therapy. Nat Commun, 2016 **7**: p. 12335. [PubMed: 27498556] **7**
48. Paulos CM, et al., Microbial translocation augments the function of adoptively transferred self/tumor-specific CD8+ T cells via TLR4 signaling. J Clin Invest, 2007 117(8): p. 2197–204. [PubMed: 17657310]
49. Grange M, et al., Activated STAT5 promotes long-lived cytotoxic CD8+ T cells that induce regression of autochthonous melanoma. Cancer Res, 2012 72(1): p. 76–87. [PubMed: 22065720]
50. Miyazaki T, et al., Functional activation of Jak1 and Jak3 by selective association with IL-2 receptor subunits. Science, 1994 266(5187): p. 1045–7. [PubMed: 7973659]
51. Leonard WJ, Mitra S, and Lin JX, Immunology: JAK3 inhibition-is it sufficient? Nat Chem Biol, 2016 12(5): p. 308–10. [PubMed: 27556128]
52. Srahna M, et al., CTLA-4 interacts with STAT5 and inhibits STAT5-mediated transcription. Immunology, 2006 117(3): p. 396–401. [PubMed: 16476059]
53. Bouvy AP, et al., T cells Exhibit Reduced Signal Transducer and Activator of Transcription 5 Phosphorylation and Upregulated Coinhibitory Molecule Expression After Kidney Transplantation. Transplantation, 2015 99(9): p. 1995–2003. [PubMed: 25769075]
54. Taylor A, et al., Glycogen Synthase Kinase 3 Inactivation Drives T-bet-Mediated Downregulation of Co-receptor PD-1 to Enhance CD8(+) Cytolytic T Cell Responses. Immunity, 2016 44(2): p. 274–86. [PubMed: 26885856]
55. Sullivan BM, et al., Antigen-driven effector CD8 T cell function regulated by T-bet. Proc Natl Acad Sci U S A, 2003 100(26): p. 15818–23. [PubMed: 14673093]

56. Martinez GJ, et al., The transcription factor NFAT promotes exhaustion of activated CD8(+) T cells. Immunity, 2015 42(2): p. 265–278. [PubMed: 25680272]
57. Vaeth M and Feske S, NFAT control of immune function: New Frontiers for an Abiding Trooper. F1000Res, 2018 7: p. 260. [PubMed: 29568499]
58. Patra AK, et al., An alternative NFAT-activation pathway mediated by IL-7 is critical for early thymocyte development. Nat Immunol, 2013 14(2): p. 127–35. [PubMed: 23263556]
59. Grange M, et al., Active STAT5 regulates T-bet and eomesodermin expression in CD8 T cells and imprints a T-bet-dependent Tc1 program with repressed IL-6/TGF-beta1 signaling. J Immunol, 2013 191(7): p. 3712–24. [PubMed: 24006458]
60. Kinter AL, et al., The common gamma-chain cytokines IL-2, IL-7, IL-15, and IL-21 induce the expression of programmed death-1 and its ligands. J Immunol, 2008 181(10): p. 6738–46. [PubMed: 18981091]
61. Fortner KA, et al., The molecular signature of murine T cell homeostatic proliferation reveals both inflammatory and immune inhibition patterns. J Autoimmun, 2017 82: p. 47–61. [PubMed: 28551033]
62. Kearl TJ, et al., Programmed death receptor-1/programmed death receptor ligand-1 blockade after transient lymphodepletion to treat myeloma. J Immunol, 2013 190(11): p. 5620–8. [PubMed: 23616570]
63. Jing W, et al., Combined immune checkpoint protein blockade and low dose whole body irradiation as immunotherapy for myeloma. J Immunother Cancer, 2015 3(1): p. 2. [PubMed: 25614821]
64. Vu MD, et al., Critical, but conditional, role of OX40 in memory T cell-mediated rejection. J Immunol, 2006 176(3): p. 1394–401. [PubMed: 16424166]
65. Arruda LCM, et al., Homeostatic proliferation leads to telomere attrition and increased PD-1 expression after autologous hematopoietic SCT for systemic sclerosis. Bone Marrow Transplant, 2018 53(10): p. 1319–1327. [PubMed: 29670207]
66. D'Souza A, et al., A Phase 2 Study of Pembrolizumab during Lymphodepletion after Autologous Hematopoietic Cell Transplantation for Multiple Myeloma. Biol Blood Marrow Transplant, 2019.
67. Overman MJ, et al., Durable Clinical Benefit With Nivolumab Plus Ipilimumab in DNA Mismatch Repair-Deficient/Microsatellite Instability-High Metastatic Colorectal Cancer. J Clin Oncol, 2018 36(8): p. 773–779. [PubMed: 29355075]
68. Chong EA, et al., PD-1 blockade modulates chimeric antigen receptor (CAR)-modified T cells: refueling the CAR. Blood, 2017 129(8): p. 1039–1041. [PubMed: 28031179]
69. Bernatchez C, et al., Effect of a novel IL-2 cytokine immune agonist (NKTR-214) on proliferating CD8+T cells and PD-1 expression on immune cells in the tumor microenvironment in patients with prior checkpoint therapy. 2017 35(15_suppl): p. 2545–2545.
70. Miller JS, et al., A First-in-Human Phase I Study of Subcutaneous Outpatient Recombinant Human IL15 (rhIL15) in Adults with Advanced Solid Tumors. Clin Cancer Res, 2018 24(7): p. 1525–1535. [PubMed: 29203590]
71. Sneller MC, et al., IL-15 administered by continuous infusion to rhesus macaques induces massive expansion of CD8+ T effector memory population in peripheral blood. Blood, 2011 118(26): p. 6845–8. [PubMed: 22067383]

Statement of significance

For optimal anti-cancer effect, T-cell therapies including CAR-T, TIL, and transgenic T-cell require transfer into lymphodepleted recipients and homeostatic activation, however, concomitant homeostatic inhibition mitigates T-cell efficacy. Checkpoint blockade uncouples homeostatic inhibition from activation, amplifying T-cell responses. Conversely, tumors non-responsive to checkpoint blockade or BMT are treatable with *immunotransplant*.

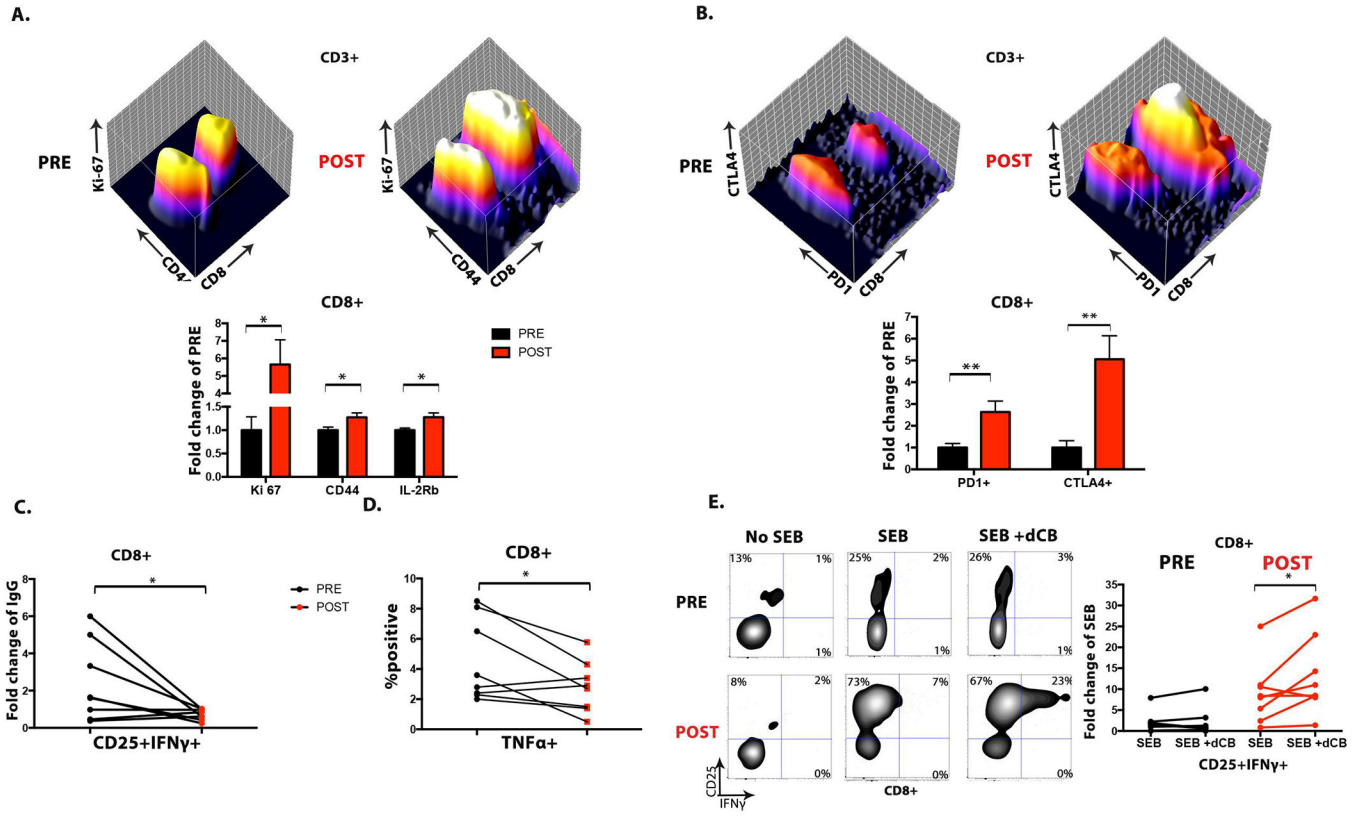

Figure 1. Homeostatic activation is coupled to homeostatic inhibition in patients receiving autologous BMT

Peripheral blood mononuclear cells (PBMCs) were isolated from patients prior to receiving BEAM (BCNU, etoposide, cytarabine, melphalan) chemotherapy – designated as 'pre-transfer' or "PRE" and – 7 to 10 days after autologous BMT, CD34-mobilized peripheral blood stem cell transplantation, and reinfusion – designated as "post-transfer" or "POST." The expression of homeostatic proliferation and activation markers **A)** Ki-67, CD44, and IL-2Rβ and **B)** checkpoint receptors CTLA4 and PD1 were assessed on CD8+ T-cells by flow cytometry.

Fold change = [MFI of POST sample] / [MFI of PRE sample per person]

PRE and POST PBMCs were cultured with 1μg plate-bound anti-CD3, 10μg plate-bound PD-L1/IgG1, and 1μg/mL of soluble anti-CD28 for 72 hours. Activation of CD8+ T-cells was assessed by **C)** extracellular CD25 and intracellular IFNγ by flow cytometry.

Fold change = [percent positive of PD-L1 sample] / [percent positive of IgG sample per person]

Similarly, PRE and POST PBMCs were cultured with 1μg plate-bound anti-CD3 and 1μg plate-bound CD80/IgG1 for 48 hours. Activation of CD8+ T-cells was assessed by **D)** intracellular TNFα production by flow cytometry.

PRE and POST PMBCs were pretreated with 10μg of ipilimumab and nivolumab *in vitro* for 48 hours. After treatment, PBMCs were co-cultured with 100ng SEB for 72 more hours. Activation of CD8+ T-cells was assessed by **E)** extracellular CD25 and intracellular IFNγ by flow cytometry.

Fold change = [percent positive SEB or SEB +dCB sample] / [percent positive of No SEB sample per person]

Data are shown as mean+/− SEM. n=8 patients. Paired t-test performed *=p<.05, **=p<.01, ***=p<.001, ****=p<.0001

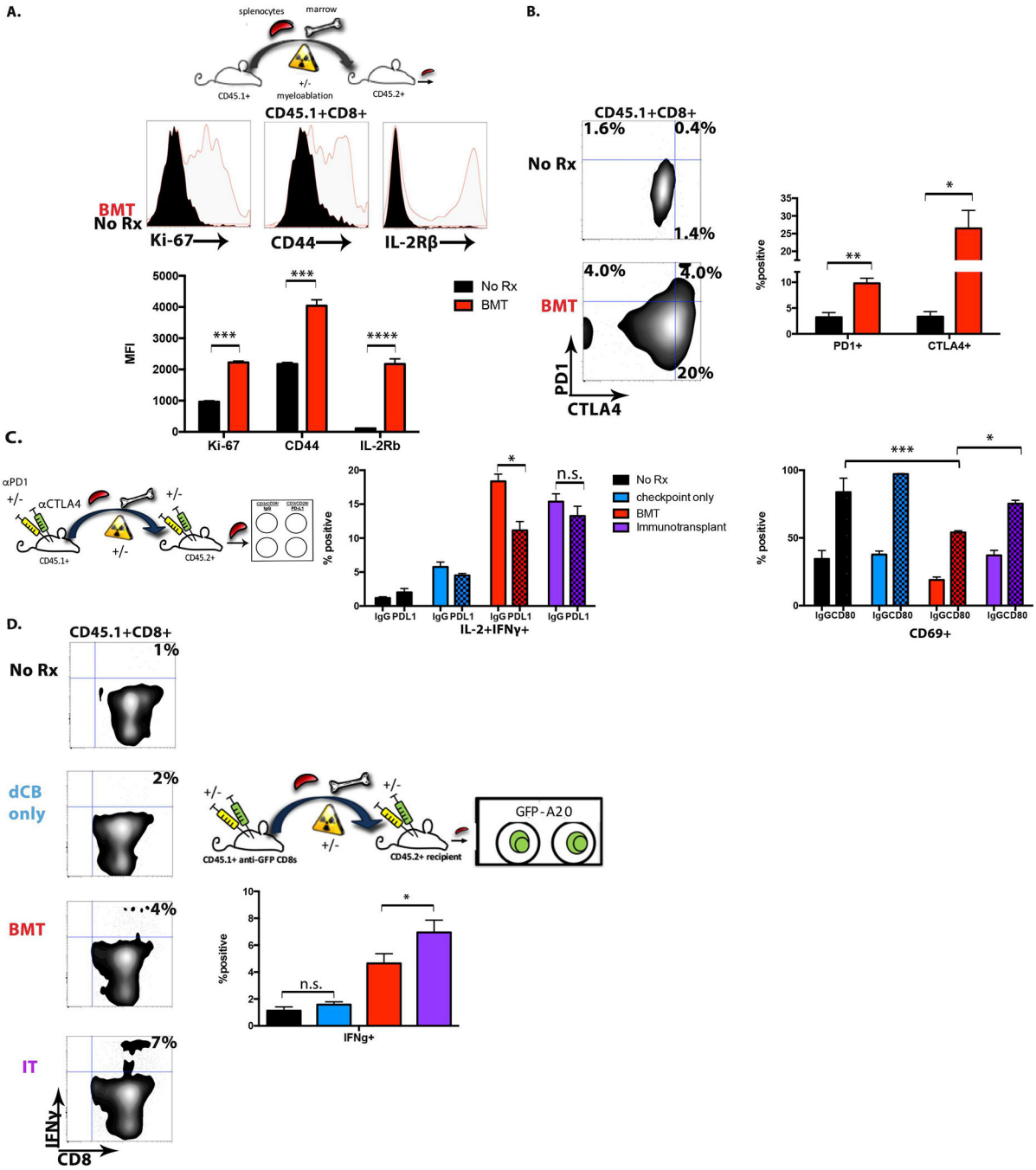

Figure 2. Homeostatic activation is coupled to homeostatic inhibition in a murine BMT model

BALB/c splenocytes were intravenously injected into the tails of congenic, syngeneic recipients that were treated with 9Gy total body irradiation (**BMT**) ■ or non-irradiated, naïve mouse (**No Rx**) ■

Seven days post-transfer, splenocytes of recipient mice were harvested and the expression of homeostatic proliferation and activation markers **A.)** Ki-67, CD44, and IL-2Rβ and **B.)** checkpoint receptors CTLA4 and PD1 on CD45.1+CD8+ T-cells were assessed by flow cytometry. Unpaired t-test was performed.

Double checkpoint blockade treatment + transfer into non-irradiated recipient mice= **antibody only (dCB only)** ■
Double checkpoint blockade treatment + transfer into irradiated recipient mice= **Immunotransplant (IT)** ■
Additionally, BALB/c donors were treated with anti-CTLA4/anti-PD1 checkpoint blockade antibodies. After treatment, donor splenocytes and bone marrow were intravenously injected into the tails of congenic recipients that had been irradiated (**IT**) or not (**dCB only**). Recipients were also treated with double checkpoint blockade as well.
Seven days post-transfer, recipient splenocytes were magnet-sorted and enriched for CD8+ T-cells then cultured with 500ng of plate-bound anti-CD3ε and 20μg PD-L1/IgG and 2μg/mL of soluble anti-CD28 for 12 or 24 hours. Activation of CD45.1+CD8+ T-cells was assessed by **C)** (*left panel*) intracellular IFNγ and IL-2 by flow cytometry.
n=6–8 mice per group from two independent experiments. Unpaired t-test was performed.
Similarly, magnet-sorted CD8+ T-cell-enriched splenocytes were cultured with 300ng of plate-bound anti-CD3ε and plate-bound 500ng of CD80/IgG for 24 hours. Activation of CD45.1+CD8+ T-cells was assessed by **C)** (*right panel*) extracellular CD69.
n=4–6 mice per group from two independent experiments. One-way ANOVA and multiple comparisons post-test performed compared to BMT+CD80.
Anti-GFP CD8+ T-cell donor mice (background F1 o were treated with double checkpoint blockade antibodies and transferred to congenic wild-type recipient mice that had or had not been irradiated. Seven days post-transfer, splenocytes were harvested and stimulated with a variant of A20 lymphoma cell line that expressed GFP. **D)** Intracellular IFNγ production was assessed by flow cytometry. Representative data shown. n=6–8 mice from two independent experiments. One-way ANOVA and multiple comparisons post-test performed compared to IT. IT was compared to ‘dCB only’ and ‘No Rx’ ***p<.001
Data are shown as mean+/− SEM. *=p<.05, **=p<.01, ***=p<.001, ****=p<.0001

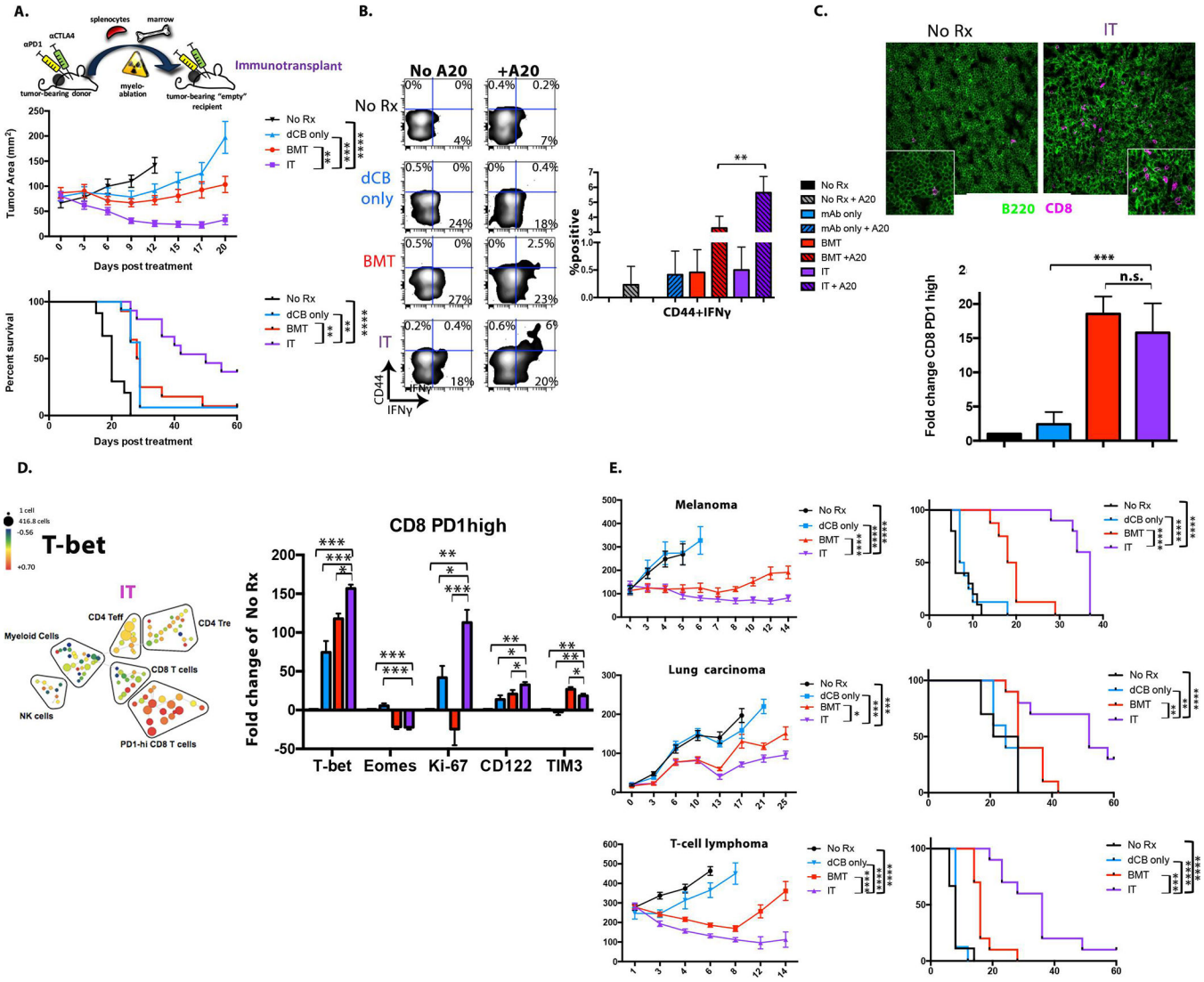

Figure 3. Immunotransplant induces tumor-specific immune responses, reverses T-cell exhaustion, and treats lymphoid and solid tumors

Donor mice were inoculated with murine B-cell lymphoma A20 cell line for 7 days then treated with anti-CTLA4/anti-PD1 checkpoint blockade. After treatment, splenocytes and bone marrow were transferred to TBI syngeneic recipient mice (Immunotransplant; **IT)** that bore the same A20 tumor; recipient mice were also treated with dCB. As controls, untreated splenocytes were transferred to irradiated recipients (**BMT**). Furthermore, tumor-bearing mice were treated with just double checkpoint blockade alone (**dCB only**) or no treatment (**No Rx).**

A) Tumor growth curve and survival curve of the mice from each group. n=11 mice per group. Two-way ANOVA performed and compared to IT.

Mice from each group were bled 11 days post-transfer or treatment start. Lymphocytes were isolated and re-stimulated in the presence of irradiated A20 tumor cells *in vitro* for 48 hours. Activation of CD8+ T-cells was assessed by **B)** intracellular IFNγ and extracellular CD44 by flow cytometry.

n=6 mice per group from two independent experiments. One-way ANOVA and multiple comparisons post-test performed compared to IT + A20. IT +A20 compared to dCB only+ A20 and No Rx + A20 ****p<.0001.

Tumors from No Rx (*left panel*) and IT (*right panel*) were harvested 7 days post-transfer, and tumor-infiltrate was assessed by **C)** *(top panel)* immunoflouresence. The activation status of tumor-infiltrating cells was assessed by mass cytometry (Cytof). **C)** *(bottom panel)* normalized number of tumor-infiltrating of $PD1^{hi}$ CD8+T-cells.

Fold change = [percentlogratio] / [average percentlogratio of No Rx]

One-way ANOVA and multiple comparisons post-test performed compared to IT

D) Activation status of $PD1^{hi}$ CD8+T-cells shown.

Fold change = [fold change] / [average fold change of No Rx]

One-way ANOVA and multiple comparisons post-test performed compared to IT

Mice bearing murine melanoma B16, lung carcinoma KLN205, and T-cell lymphoma EL4 tumors were treated as previously described. **E)** Graph showing tumor growth curve and survival curve. n=8–12 mice per group. Two-way ANOVA and multiple comparisons post-test performed compared to IT.

Data are shown as mean+/− SEM. *=p<.05, **=p<.01, ***=p<.001, ****=p<.0001

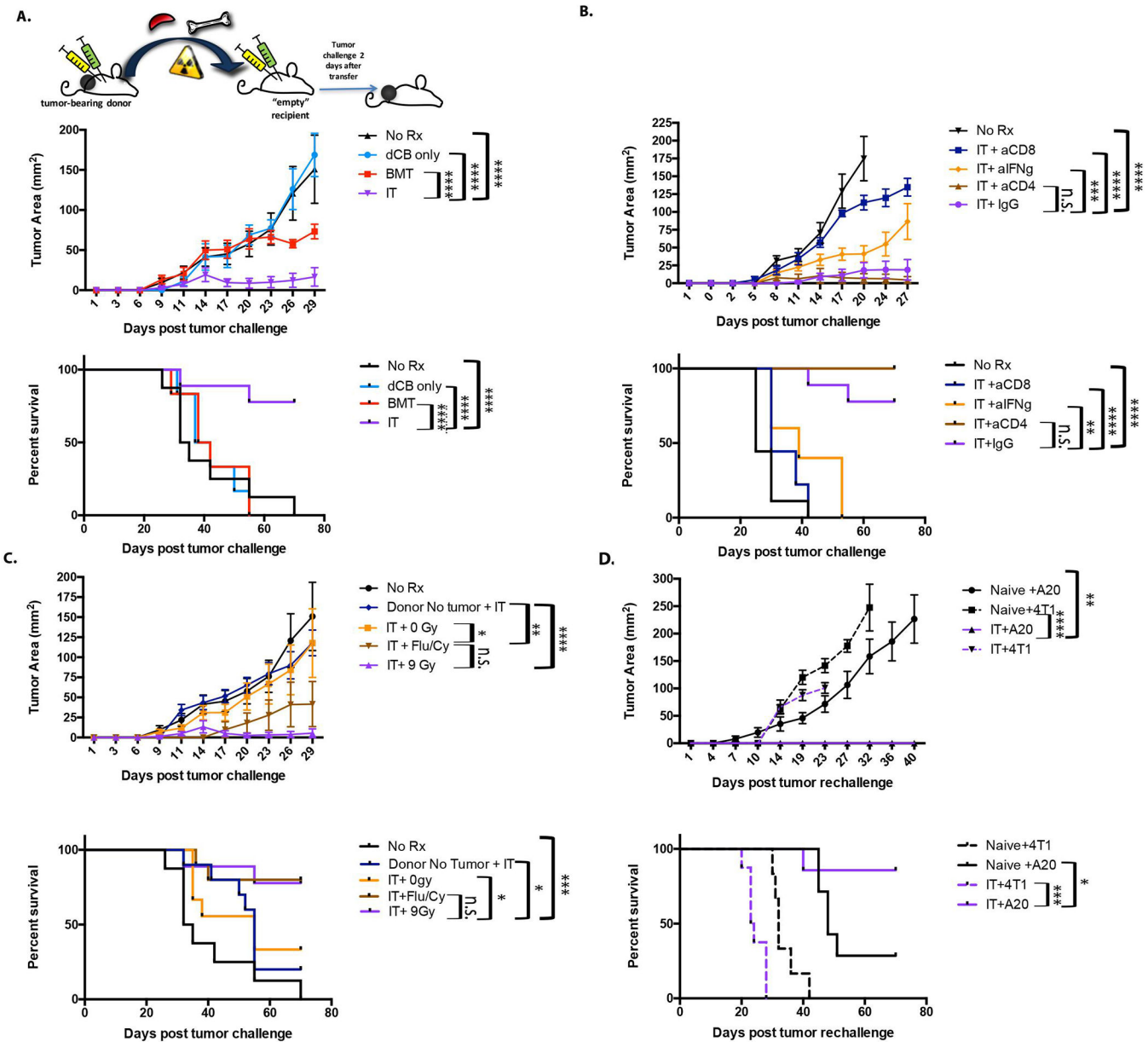

Figure 4 –. Immunotransplant anti-tumor immunity is CD8-, IFNγ- and lymphodepletion-dependent

All of the previously described therapies (No Rx, dCB only, BMT, IT) were performed with the exception that, at the time of transfer, all recipient mice were not tumor-bearing. All recipient mice were tumor-challenged with A20 two days post-transfer or post-treatment initiation. **A)** Tumor growth curve and survival curve of the mice from each group. n=9–11 mice per group. Two-way ANOVA was performed and compared to IT.

Key effectors of IT anti-tumor immunity were assessed by treating IT-treated recipients with depleting CD8 (IT +αCD8), CD4 (IT +αCD4), IFNγ (IT +αIFNγ) antibodies before and after splenocyte transfer. **B)** Graph showing tumor growth curve and survival curve. n=9–12 mice per group. Two-way ANOVA was performed and multiple comparisons post-test performed compared to compared to IT+ IgG control.

Additionally, IT mice were treated as described, but the donor lacked the A20 tumor (Donor No Tumor + IT), or the recipient mouse was not irradiated (IT+ 0Gy) or was lymphodepleted with chemotherapy fludarabine/cyclcophosphamide instead of TBI (IT+ Flu/Cy). **C)** Graph showing tumor growth curve and survival curve. n=8–12 mice per group. Two-way ANOVA and multiple comparisons post-test performed compared to IT+ Flu/Cy. After IT-treated mice had cleared the A20 tumor, recipient mice were re-challenged with the same A20 tumor cells or 4T1 breast tumor cells. **D)** Graph showing tumor growth curve and survival curve. n=6–8 mice per group. Two-way ANOVA and multiple comparisons post-test performed compared to IT+ A20.

Data are shown as mean+/− SEM. *=p<.05, **=p<.01, ***=p<.001, ****=p<.0001

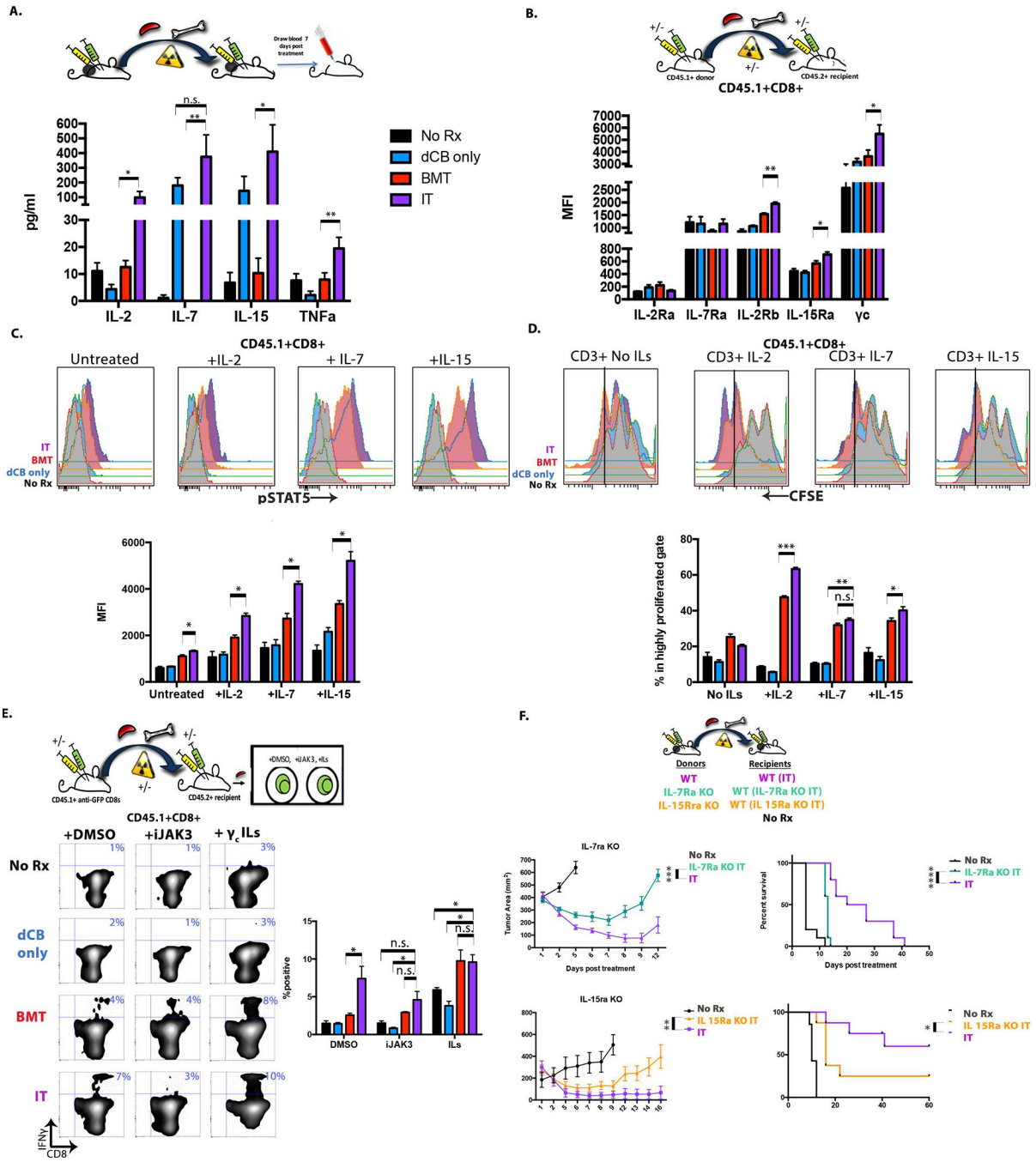

Figure 5. γ_C cytokine signaling is amplified by immunotransplant and necessary for anti-tumor immunity

Serum was isolated from mice of each therapy group and **A**) cytokine levels were assessed by bead-based multiplex assay Luminex® platform. One-way ANOVA was performed and compared to IT. n=6–9 mice per group from two independent experiments.

BALB/c donor mice were treated with anti-CTLA4/anti-PD1 checkpoint blockade antibodies, and splenocytes were harvested and intravenously injected into congenic recipient mice that had received total body radiation (modeling IT). As controls, anti-CTLA4/anti-PD1 checkpoint blockade-treated congenic splenocytes were also intravenously

injected into recipients that had not received TBI (modeling dCB only); additionally, splenocytes of untreated donor mice were transferred into recipients that had not received TBI (modeling No Rx) or TBI recipients (modeling BMT). Three days post-transfer, recipient splenocytes were harvested and **B)** the expression of common gamma chain (γ_c) receptor subunits was assessed by flow cytometry. One-way ANOVA was performed and compared to IT. n=8 mice per group from two independent experiments.

Splenocytes from each group were stimulated *in vitro* with 100ng of recombinant IL-2, IL-7, or IL-15 for 20 minutes. Activation and downstream signaling was measured by **C)** nuclear phospho-STAT5 (Y694) levels assessed by flow cytometry. One-way ANOVA and multiple comparisons post-test performed compared to IT. n=8 mice per group from two independent experiments.

Splenocytes from each group were labelled with CFSE and treated *in vitro* with soluble 100ng of anti-CD3e and 100ng of recombinant IL-2, IL-7, or IL-15 for 48 hours. Proliferation was assessed by **D)** CFSE dilution. One-way ANOVA was performed and multiple comparisons post-test performed compared to IT. n=6 mice per group from two independent experiments.

GFP-specific CD8 donor mice were treated with anti-CTLA4/anti-PD1 double checkpoint blockade antibodies and intravenously injected into congenic recipients that had been irradiated. Splenocytes were harvested 7 days post-transfer and stimulated *in vitro* with GFP-expressing A20 cells in the presence of DMSO, JAK3-specific inhibitor tofacitinib (iJAK3), or a mix of 100ng recombinant IL-2, IL-7 and IL-15. Activation was assessed by **E)** intracellular IFNγ production. n=7–8 mice per group from two independent experiments.

Donor mice whose lymphocytes had been engineered to lack IL-7Rα (B6 IL-7Rα KO IT) or IL-15Rα (B6.129 IL-15Rα KO), or wild-type mice were inoculated with T-cell lymphoma EL4 tumor then treated with anti-CTLA4/anti-PD1 checkpoint blockade antibodies. After treatment, splenocytes and bone marrow were transferred to TBI syngeneic recipient mice that bore the same EL4 tumor. **F)** Graph showing tumor growth and survival. Two-way ANOVA and multiple comparisons post-test performed compared to IT.

Data are shown as mean+/− SEM. *=p<.05, **=p<.01, ***=p<.001, ****=p<.0001

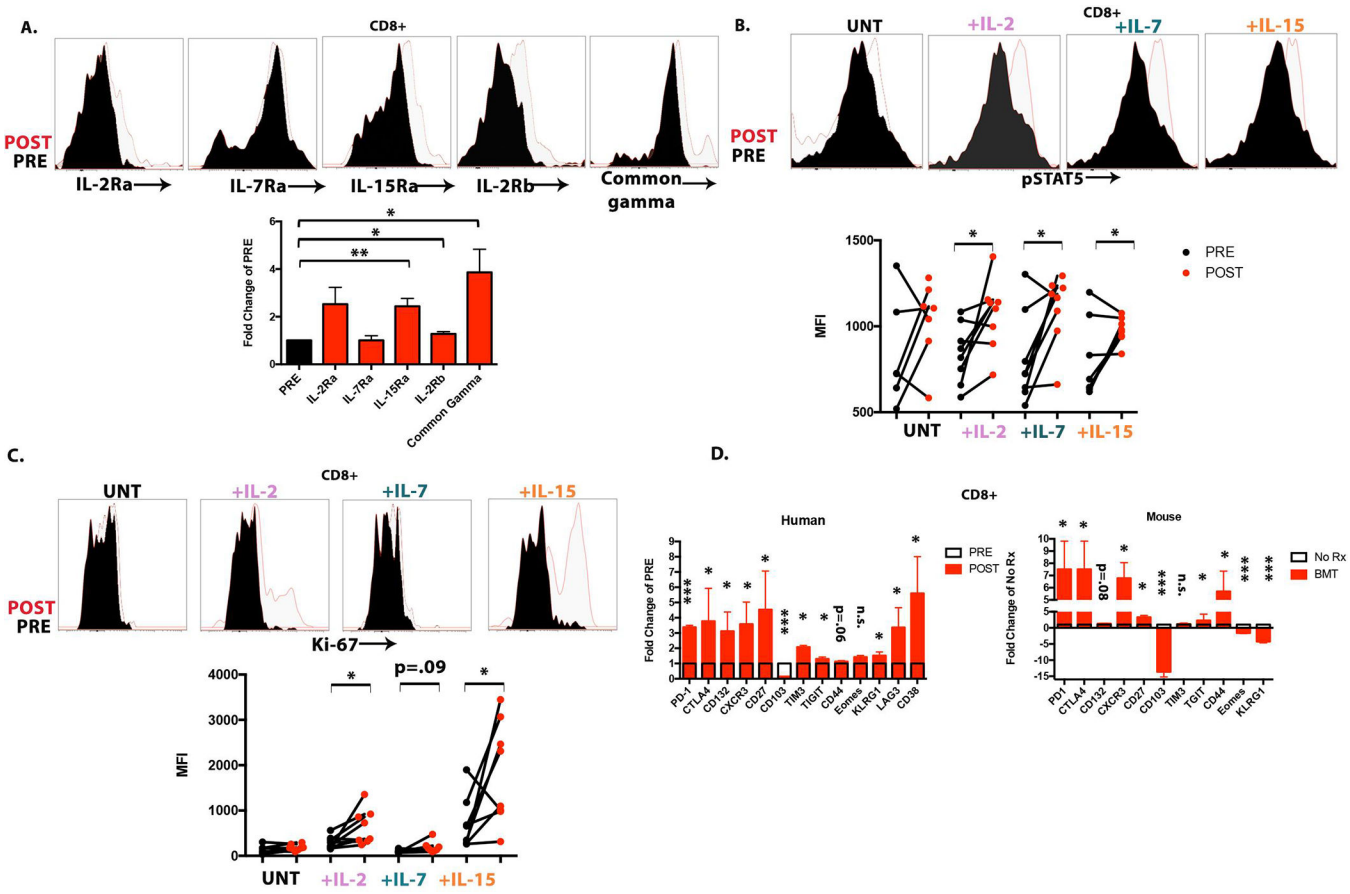

Figure 6. BMT increases γ_c receptor and signaling on donor T-cells in lymphoma patients

The expression of **A)** γ_C receptor subunits was assessed by flow cytometry on patients' PRE and POST transplant on CD8+T-cells. n=8 patients. Paired t-test was performed.

PRE and POST PBMCs were stimulated *in vitro* with recombinant IL-2, IL-7 and IL-15. Activation and downstream signaling were determined by **B)** nuclear phospho-STAT5 (Y694) levels, and proliferative capability was assessed by **C)** Ki-67 levels gated on CD8+ T-cells. n=8 patients. Paired t-test was performed.

The activation status of PRE and POST PBMCs was assessed by Cytof. **D)** Graph (on left) showing the expression of several markers on patients' CD8+ T-cells by Cytof. For comparison, the activation status of splenocytes in No Rx- and BMT-treated mice were assessed by Cytof (on right). N=4 patients. Paired t-test was performed. N=3 mice per group. Unpaired t-test was performed.

Fold Change of PRE* = [Raw fold change of POST] / [Raw fold change of PRE per person]

Fold Change of No Rx* = [Fold change of BMT] / [Average fold change of No Rx]

* Except for CLTA-4, PD1, CD27. Fold change = [[Count of BMT CD8+ T-cells positive]/ [Total CD8+ T-cell per person or per mouse]] / [Count of PRE or No Rx CD8+ T-cells positive]/ [Total CD8+ T-cell per person or per mouse]]

Data are shown as mean+/− SEM. *=p<.05, **=p<.01, ***=p<.001, ****=p<.0001

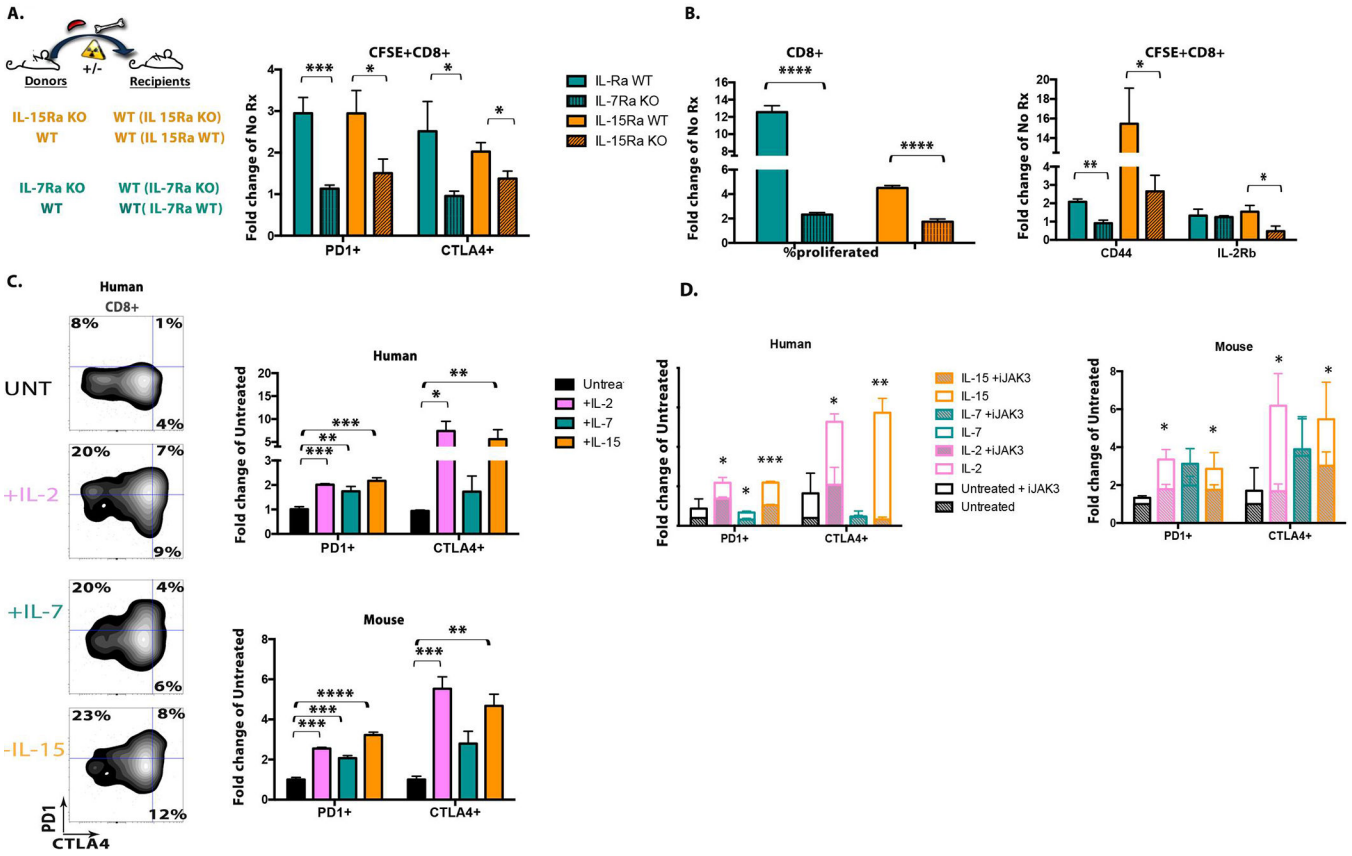

Figure 7. MT and γ_c cytokines induce JAK3-dependent homeostatic activation and inhibition

Splenocytes from IL-7Rα KO and IL-15Rα KO and their wildtype counterpart were labelled with CFSE and intravenously injected into recipients that had been treated with TBI or not. Five days post-transfer, splenocytes were harvested and **A)** PD1 and CTLA4 **B)** Ki-67, CD44, and IL-2Rβ on CFSE+ CD8+ T-cells were assessed by flow cytometry. n=6–8 mice from two independent experiments. Unpaired t-test was performed.

PMBCs from healthy human donors or splenocytes from naïve mice were stimulated with 100ng of recombinant IL-2, IL-7 and IL-15 for 4 days. The expression of **C)** PD1 and CTLA4 human and mouse CD8+ T-cells was assessed by flow cytometry. n=6 healthy donors from two independent experiments. n=6 mice from two independent experiments. Unpaired t-test was performed.

PMBCs from healthy human donors or splenocytes from naïve mice were stimulated *in vitro* with 100ng of recombinant IL-2, IL-7 and IL-15 and also in the presence of 1uM JAK3-specific inhibitor tofacitinib (iJAK3). The expression of **D)** PD1 and CTLA4 on human and mouse CD8+ T-cells was assessed by flow cytometry. n=6 healthy donors from two independent experiments. n=6 mice from two independent experiments. Unpaired t-test was performed.

Data are shown as mean+/− SEM. *=p<.05, **=p<.01, ***=p<.001, ****=p<.0001